MOX-Report No. 10/2025

Stability and interpolation estimates of Hellinger-Reissner virtual element spaces

Botti, M.; Mascotto, L.; Vacca, G.; Visinoni, M.

MOX, Dipartimento di Matematica
Politecnico di Milano, Via Bonardi 9 - 20133 Milano (Italy)

mox-dmat@polimi.it https://mox.polimi.it

Stability and interpolation estimates of Hellinger–Reissner virtual element spaces

Michele Botti[*], Lorenzo Mascotto[†], Giuseppe Vacca[‡], Michele Visinoni[*]

Abstract

We prove stability and interpolation estimates for Hellinger–Reissner virtual elements; the constants appearing in such estimates only depend on the aspect ratio of the polytope under consideration and the degree of accuracy of the scheme. We further investigate numerically the behaviour of the constants appearing in the stability estimates on sequences of badly-shaped polytopes and for increasing degree of accuracy.

AMS subject classification: 65N12; 65N30.

Keywords: virtual element method; stability estimate; interpolation estimate; Hellinger–Reissner principle.

1 Introduction

State-of-the-art. Virtual elements were introduced more than a decade ago [8] as a generalization of finite elements able to handle meshes of polytopic elements; different types of elements have been designed for several problems, including the linear elasticity problem based on the Hellinger–Reissner (HR) principle. A lowest order HR virtual element in 2D was introduced in [5] and generalized to the arbitrary order case in [6]; the 3D version of the method is presented in [17, 31]. HR virtual elements consist of strongly symmetric stresses, whose degrees of freedom are associated with the interior of a d dimensional element and its $d-1$ dimensional facets, $d = 2, 3$, and piecewise polynomial displacements.

The literature of finite elements involving strongly symmetric stresses traces back to the end of the 60ies: Watwood and Hartz [32] constructed lowest order spaces of strongly symmetric stresses on triangular meshes; therein, there are no vertex degrees of freedom and the design of the element hinges on a suitable split of each triangle into three smaller triangles. That method was analyzed by Hlaváček [24], and Johnson and Mercier [26]. Henceforth, we shall be referring to that kind of element as JM element. The JM element was generalized to the 3D case by Krizek [27]. A different avenue was undertaken decades later by Arnold and Winther [4] (AW) for triangular meshes; no elemental splits are there necessary, the price to pay being an increase of the dimension of local spaces and the use of vertex degrees of freedom. The AW original approach was generalized to rectangular meshes in [2, 14] and 3D elements in [1, 3]. We also mention the work by Hu and Zhang [25] for polynomial order larger than 4 on tetrahedral meshes, which was employed by Chen and Huang to construct a full elasticity complex in [13]. Other elasticity complexes based on Alfeld and Worsey-Farin splits are discussed in [15, 21]. More recently, JM elements in any dimension were designed in [22].

To the best of our understanding, the above references can be clustered into two main categories: AW types elements, whose design does not require any split of the mesh elements but in d dimensions is based on degrees of freedom on all geometrical entities with finite nonzero ℓ-dimensional Hausdorff measure for all $\ell = 0, \dots, d$; JM types elements, which compared to AW

[*]MOX, Department of Mathematics, Politecnico di Milano, 20133 Milano, Italy (michele.botti@polimi.it, michele.visinoni@polimi.it)

[†]Department of Mathematics and Applications, University of Milano–Bicocca, 20125 Milan, Italy; Faculty of Mathematics, University of Vienna, 1090 Vienna, Austria; IMATI-CNR, 27100 Pavia, Italy (lorenzo.mascotto@unimib.it)

[‡]Department of Mathematics, University of Bari, 70125 Bari (giuseppe.vacca@uniba.it)

elements need fewer degrees of freedom attached only to geometrical entities with codimension 0 and 1, but require some elemental splits for their design.

HR virtual element spaces retain advantages of AW and JM finite elements: no split of the mesh elements is necessary for their design; the degrees of freedom are only attached to the interior and the facets of an element; they support meshes of polytopic elements.

These upsides come at the price that discrete functions are not known in closed form, but only through certain polynomial projections on the skeleton of the mesh and the interior of each mesh element. As such, the bilinear forms appearing in the weak formulation of the linear elasticity problem in mixed formulation are not computable for HR virtual element tensors. For this reason, following the standard virtual element gospel [8], bilinear forms are discretized so as to be the sum of two terms: one guaranteeing the polynomial consistency of the method and requiring a projection of the HR virtual element tensors onto polynomial tensors; the other providing stability, i.e., well-posedness of the linear system equivalent to the method.

Goals. In the literature on HR virtual elements [5, 6, 17, 31], several stabilizations have been employed and heuristic arguments as for its scaling with respect to local L^2 inner products are discussed. In this paper, we show rigorous results along this directions: for standard geometries, we exhibit stabilizations with correct scaling properties, and stability constants in the sense of (20) below, which only depend on the shape-regularity of the mesh and the degree of accuracy of the scheme. The technical tools we employ boil down to integration by parts, polynomial inverse inequalities, direct estimates, polynomial approximation results, and well-posedness results of mixed formulation with certain boundary conditions.

Another important theoretical aspect in the analysis of virtual elements is the derivation of interpolation estimates, with constants that are explicit with respect to the shape of the polytopic elements. Such estimates, yet with implicit constants, are already available for the 2D lowest order case [5] and they can be generalized to the general order and 3D cases as remarked in [6, 17, 31]. Here, we provide a new proof of interpolation estimates in HR virtual elements (with explicit constants) based on using the stability estimates discussed above.

As we derive stability and interpolation estimates for standard geometries (star-shaped elements with no small facets) and for a fixed degree of accuracy, the question arises naturally whether the proven bounds are effectively robust with those respects. Thus, we investigate numerically the behaviour of the stability constants on sequences of badly-shaped elements and for increasing degree of accuracy.

Notation. Given a domain D in $\mathbb{R}^d$, $d = 2, 3$, with boundary ∂D, outward unit normal vector $\mathbf{n}_D$, and diameter h_D, $L^2(D)$ is the space of square integrable functions over D and $L^2_0(D)$ is its subspace of functions with zero average over D. $H^s(D)$ denotes the Sobolev space of order s in $\mathbb{N}$; we consider fractional order spaces defined by interpolation theory. $H^1_0(D)$ denotes the subspace of $H^1(D)$ consisting of functions with zero trace over the boundary of D. We endow each Sobolev space with seminorm, norm, and bilinear forms

$$|\cdot|_{s,D}, \qquad \|\cdot\|_{s,D}, \qquad (\cdot,\cdot)_{s,D}.$$

The negative order Sobolev space $H^{-1}(D)$ are defined as the dual space of $H^1_0(D)$ and endowed with the norm

$$\|v\|_{-1,D} := \sup_{\phi\in H^1_0(D),\, |\phi|_{1,D}\neq 0} \frac{{}_{-1}\langle v,\phi\rangle_{1,D}}{|\phi|_{1,D}} \qquad \forall v \in H^{-1}(D). \tag{1}$$

Vector and tensor valued Sobolev and Lebesgue spaces are defined similarly, and are denoted by replacing H and L by $\mathbf{H}$ and $\mathbb{H}$, and $\mathbf{L}$ and $\mathbb{L}$; vector fields are highlighted in boldface font, and tensors are further underlined (e.g., v, $\mathbf{v}$, and $\underline{\mathbf{v}}$). On most occasions, Roman and Greek letters will be employed for vectors and tensors, respectively.

We usual standard notation for differential operators. In particular, $\nabla_S\cdot$ and $\mathbf{div}\,\cdot$ are the symmetric gradient of a vector field and the divergence operator of a tensor. We further define the space $\mathbb{H}^s_{\mathcal{S}}(\mathbf{div}, D)$, $s \geq 0$, of $\mathbb{H}^s(D)$ symmetric tensors $\underline{\boldsymbol{\sigma}}$ such that $\mathbf{div}\,\underline{\boldsymbol{\sigma}}$ is in $\mathbf{H}^s(D)$. We simply

write $\mathbb{H}(\mathbf{div}, D)$ if $s = 0$. For tensors $\underline{\boldsymbol{\sigma}}$ in $\mathbb{H}^s_{\mathcal{S}}(\mathbf{div}, D)$, the image space of the map (called trace operator) that associates $\underline{\boldsymbol{\sigma}}$ with $\underline{\boldsymbol{\sigma}}_{|\partial D}\,\mathbf{n}_D$ is called $\mathbf{H}^{-\frac{1}{2}}(\partial D)$, which we endow with the norm

$$\|\underline{\boldsymbol{\sigma}}\mathbf{n}_D\|_{-\frac{1}{2},\partial D} := \sup_{\mathbf{v}\in\mathbb{H}^1(D),\ \|\mathbf{v}\|_{1,D}\neq 0} \frac{(\underline{\boldsymbol{\sigma}}, \nabla\mathbf{v})_{0,D} + (\mathbf{div}\,\underline{\boldsymbol{\sigma}}, \mathbf{v})_{0,D}}{h_D^{-\frac{1}{2}}\|\mathbf{v}\|_{0,\partial D} + |\mathbf{v}|_{\frac{1}{2},\partial D}}.$$

The trace operator above is surjective, see, e.g., [10, Lemma 2.1.2], and continuous: there exists a positive c_{tr} only depending on the shape of D such that

$$\|\underline{\boldsymbol{\sigma}}\mathbf{n}_D\|_{-\frac{1}{2},\partial D} \le c_{tr}(h_D^{-1}\|\underline{\boldsymbol{\sigma}}\|_{0,D} + \|\mathbf{div}\,\underline{\boldsymbol{\sigma}}\|_{0,D}) \qquad \forall\underline{\boldsymbol{\sigma}} \in \mathbb{H}^s_{\mathcal{S}}(\mathbf{div}, D). \tag{2}$$

The constant c_{tr} coincides with the constant appearing in the right-inverse trace inequality; see, e.g., [29, Theorem 3.37]. We denote the duality pairing between $H^{-\frac{1}{2}}(\partial D)$ and $H^{\frac{1}{2}}(\partial D)$ by $\langle\cdot,\cdot\rangle$.

Given $\mathbb{I}$ the identity tensor, we introduce $\mathbf{dev}\,\underline{\boldsymbol{\sigma}} = \underline{\boldsymbol{\sigma}} - d^{-1}\,\mathrm{tr}(\underline{\boldsymbol{\sigma}})\mathbb{I}$. $\mathrm{P}_p(D)$ represents the space of polynomials of maximum degree p in $\mathbb{N}$ over D. We use the convention $\mathrm{P}_{-1}(D) = \{0\}$. Vector and tensor polynomial spaces are denoted by replacing P with $\mathbf{P}$ and $\mathbb{P}$. The space of rigid body motions

$$\mathbf{RM}(D) := \{\mathbf{r}(\mathbf{x}) = \boldsymbol{\alpha} + \boldsymbol{\omega}\wedge\mathbf{x} \mid \boldsymbol{\alpha}\in\mathbb{R}^3,\ \boldsymbol{\omega}\in\mathbb{R}^3\}$$

has dimension six and is spanned by

$$(1,0,0);\qquad (0,1,0);\qquad (0,0,1);\qquad (1,0,0)\wedge\mathbf{x};\qquad (0,1,0)\wedge\mathbf{x};\qquad (0,0,1)\wedge\mathbf{x}.$$

For positive constants a and b, we write $a \lesssim b$ if there exists a uniform positive constant c such that $a \le c\ b$. If $a \lesssim b$ and $b \lesssim a$, we write $a \approx b$. On relevant occasions, we shall pinpoint the actual dependence of the hidden constant.

The model problem. In what follows, we focus on 3D problems only, albeit the forthcoming analysis can be generalized to the 2D case with minor modifications. Given a Lipschitz polyhedral domain Ω in $\mathbb{R}^3$ with boundary $\Gamma := \partial\Omega$, a symmetric, uniformly elliptic elasticity tensor $\mathbb{D} = \mathbb{C}^{-1} : \mathbb{R}^{3\times3} \to \mathbb{R}^{3\times3}$ on the space of symmetric 3×3 matrices, and $\mathbf{f}$ in $\mathbf{L}^2(\Omega)$, we consider the linear elasticity problem: Find $\mathbf{u} : \Omega \to \mathbb{R}^3$ such that

$$\begin{cases} -\,\mathbf{div}\ \underline{\boldsymbol{\sigma}} = \mathbf{f} & \text{in } \Omega \\ \underline{\boldsymbol{\sigma}} = \mathbb{C}\nabla_S(\mathbf{u}) & \text{in } \Omega \\ \underline{\boldsymbol{\sigma}}\mathbf{n} = \mathbf{0} & \text{on } \partial\Omega. \end{cases} \tag{3}$$

In the standard isotropic elasticity case, given nonnegative Lamé moduli $\lambda \ge 0$ and $\mu > 0$, we have

$$\mathbb{C}\underline{\boldsymbol{\tau}} := 2\mu\,\mathbf{dev}(\underline{\boldsymbol{\tau}}) + \frac{2\mu+3\lambda}{3}\,\mathrm{tr}(\underline{\boldsymbol{\tau}})\mathbb{I}, \qquad \mathbb{D}\underline{\boldsymbol{\tau}} := \frac{\mathbf{dev}(\underline{\boldsymbol{\tau}})}{2\mu} + \frac{\mathrm{tr}(\underline{\boldsymbol{\tau}})\mathbb{I}}{3(2\mu+3\lambda)}. \tag{4}$$

We introduce the spaces and inner product

$$\begin{aligned} &\mathbf{V} := \{\mathbf{v}\in\mathbf{L}^2(\Omega) \mid (\mathbf{v},\mathbf{r})_{0,\Omega} = 0 \quad \forall\mathbf{r}\in\mathbf{RM}(\Omega)\},\\ &\underline{\mathbf{\Sigma}} := \{\underline{\boldsymbol{\tau}}\in\mathbb{H}_{\mathcal{S}}(\mathbf{div},\Omega) \mid \langle\underline{\boldsymbol{\tau}}\,\mathbf{n},\mathbf{v}\rangle = 0 \quad \forall\mathbf{v}\in\mathbf{H}^1(\Omega)\}, \qquad a(\underline{\boldsymbol{\sigma}},\underline{\boldsymbol{\tau}}) := (\mathbb{D}\underline{\boldsymbol{\sigma}},\underline{\boldsymbol{\tau}})_{0,\Omega} \quad \forall\underline{\boldsymbol{\sigma}},\underline{\boldsymbol{\tau}}\in\underline{\mathbf{\Sigma}}. \end{aligned} \tag{5}$$

We endow the space $\mathbf{V}$ with $\|\cdot\|_{\mathbf{V}}$, which is the usual L^2 norm, and $\underline{\mathbf{\Sigma}}$ with the norm given by

$$\|\cdot\|^2_{\underline{\mathbf{\Sigma}}} := \|\cdot\|^2_{0,\Omega} + h_\Omega^2\|\mathrm{div}\,\cdot\|^2_{0,\Omega}.$$

The HR weak formulation of (3) is

$$\begin{cases} \text{Find } (\underline{\boldsymbol{\sigma}},\mathbf{u})\in\underline{\mathbf{\Sigma}}\times\mathbf{V} \text{ such that} \\ a(\underline{\boldsymbol{\sigma}},\underline{\boldsymbol{\tau}}) + (\mathbf{div}\,\underline{\boldsymbol{\tau}},\mathbf{u})_{0,\Omega} = 0 & \forall\underline{\boldsymbol{\tau}}\in\underline{\mathbf{\Sigma}} \\ (\mathbf{div}\,\underline{\boldsymbol{\sigma}},\mathbf{v})_{0,\Omega} = -(\mathbf{f},\mathbf{v})_{0,\Omega} & \forall\mathbf{v}\in\mathbf{V}. \end{cases} \tag{6}$$

Theorem A.7 below guarantees that problem (6) is well-posed even for inhomogeneous essential boundary conditions, with a priori bounds

$$\|\underline{\boldsymbol{\sigma}}\|_{\underline{\mathbf{\Sigma}}} + \|\mathbf{u}\|_{\mathbf{V}} \leq C\|\mathbf{f}\|_{0,\Omega}.$$

Above, C is a positive constant, which only depends on the ratio between the diameter of Ω and the radius of the largest ball contained in Ω. If other types of boundary conditions are considered, then the well-posedness of the problem can be found, e.g., in [10, Chapter 8]; in this case, we are not able to provide an explicit dependence for the stability constant.

Regular meshes of polytopic elements. Henceforth, we focus on three dimensional domains. Even though the forthcoming analysis is only concerned with local stability and interpolation estimates, we discuss regularity assumptions for given meshes of polytopic elements, as the results we shall discuss can be used in the analysis of virtual elements for problem (6) below.

Given X either an edge, facet, or polyhedron, we introduce its diameter h_X, centroid $\mathbf{x}_X$, and measure $|X|$. Given K a polyhedron, its set of facets is $\mathcal{F}^K$ and the outward unit normal vector is $\mathbf{n}^K$. Given F a facet of the mesh, its set of edges is $\mathcal{E}^F$.

We consider sequences of regular meshes $\{\mathcal{T}_n\}$ of polytopic elements in the following sense: there exists a positive ρ such that, for all meshes $\mathcal{T}_n$ in the sequence,

- each K in $\mathcal{T}_n$ is star-shaped with respect to a ball of radius larger than or equal to ρh_K;
- for each K in $\mathcal{T}_n$, each facet F in $\mathcal{F}^K$ is star-shaped with respect to a disk of radius larger than or equal to ρh_F, and is such that h_F is larger than or equal to ρh_K;
- for each K in $\mathcal{T}_n$ and F in $\mathcal{F}^K$, every edge e in $\mathcal{E}^F$ is such that h_e is larger than or equal to ρh_F.

The above assumptions may be relaxed; yet, we stick to the above setting for the presentation's sake. Henceforth, given the Lamé parameters λ and μ as in (4), we assume that

$$\lambda \text{ and (consequently) } \mu \text{ in (4) are piecewise constant over any mesh in } \{\mathcal{T}_n\}. \tag{7}$$

For future convenience, we expand the bilinear form $a(\cdot,\cdot)$ into a sum of local contribution over the elements of a mesh $\mathcal{T}_n$:

$$a(\underline{\boldsymbol{\sigma}},\underline{\boldsymbol{\tau}}) = \sum_{K\in\mathcal{T}_n} a^K(\underline{\boldsymbol{\sigma}},\underline{\boldsymbol{\tau}}) := \sum_{K\in\mathcal{T}_n} (\mathbb{D}\underline{\boldsymbol{\sigma}},\underline{\boldsymbol{\tau}})_{0,K}. \tag{8}$$

Outline of the paper. In Section 2, we introduce HR type virtual elements and discretize L^2-type inner products using polynomial projections and stabilizing bilinear forms. In Section 3, we discuss stability bounds, which we use in Section 4 to derive interpolation estimates in HR VE spaces. We assess numerically the behaviour of the stabilizations on sequences of badly-shaped elements and for increasing degree of accuracy in Section 5. Conclusions are drawn in Section 6, while technical results from the PDE theory are investigated in Appendix A.

2 Hellinger–Reissner virtual element spaces and forms

We review the construction of HR virtual elements, the choice of suitable degrees of freedom, the definition of certain polynomial spaces and polynomial projections, and the design of the discrete bilinear forms.

Polynomial spaces. We introduce the space of vector polynomials that are orthogonal in $L^2(K)$ to rigid body motions:

$$\mathbf{RM}_p^\perp(K) := \{\mathbf{q}_p \in \mathbf{P}_p(K) \mid (\mathbf{q}_p,\mathbf{r})_{0,K} = 0 \quad \forall \mathbf{r} \in \mathbf{RM}(K)\}$$

and note that

$$\mathbf{P}_p(K) = \mathbf{RM}(K) \oplus_{\mathbf{L}^2(K)} \mathbf{RM}_p^\perp(K). \tag{9}$$

For all elements K in $\mathcal{T}_n$, we further introduce the space

$$\mathbb{T}_p(K) := \{\mathbb{C}\nabla_S(\mathbf{q}_{p+1}) \mid \mathbf{q}_{p+1} \in \mathbf{P}_{p+1}(K)\}. \tag{10}$$

Virtual element spaces. Given an element K of $\mathcal{T}_n$ and p in $\mathbb{N}$, we define the Hellinger–Reissner virtual element space

$$\underline{\boldsymbol{\Sigma}}_h(K) := \{\underline{\boldsymbol{\sigma}}_h \in \mathbb{H}_{\mathcal{S}}(\mathbf{div}, K) \mid \underline{\boldsymbol{\sigma}}_h \text{ solves weakly (11) below}\},$$

where

$$\begin{cases} \underline{\boldsymbol{\sigma}}_h = \mathbb{C}\nabla_S(\mathbf{w}^*) & \\ \mathbf{div}\,\underline{\boldsymbol{\sigma}}_h = \mathbf{q}_p \in \mathbf{P}_p(K) & \text{for some vector field } \mathbf{w}^*. \\ \underline{\boldsymbol{\sigma}}_h \mathbf{n}^K{}_{|F} = \mathbf{q}_p^F \in \mathbf{P}_p(F) \quad \forall F \in \mathcal{F}^K & \end{cases} \tag{11}$$

Given $a^K(\cdot,\cdot)$ as in (8), the discrete tensor $\underline{\boldsymbol{\sigma}}_h$ defined in (11) solves

$$\begin{cases} \text{Find } \underline{\boldsymbol{\sigma}}_h \in \mathbb{H}_{\mathcal{S}}(\mathbf{div}, K),\ \mathbf{w}^* \in \mathbf{L}^2(K) \text{ such that} & \\ a^K(\underline{\boldsymbol{\sigma}}_h, \underline{\boldsymbol{\tau}}) + (\mathbf{div}\,\underline{\boldsymbol{\tau}}, \mathbf{w}^*)_{0,K} = 0 & \forall \underline{\boldsymbol{\tau}} \in \mathbb{H}_{\mathcal{S}}(\mathbf{div}, K) \\ (\mathbf{div}\,\underline{\boldsymbol{\sigma}}_h, \mathbf{z}^*)_{0,K} = (\mathbf{q}_p, \mathbf{z}^*)_{0,K} & \forall \mathbf{z}^* \in \mathbf{L}^2(K) \\ \underline{\boldsymbol{\sigma}}_h \mathbf{n}^K{}_{|F} = \mathbf{q}_p^F & \forall F \in \mathcal{F}^K. \end{cases} \tag{12}$$

Since the displacement $\mathbf{w}^*$ in (12) is unique up to rigid body motions, we fix it so as to be L^2-orthogonal to $\mathbf{RM}(K)$.

Since $\mathbb{C}$ is a constant tensor over K, see (7), the space $\mathbb{T}_p(K)$ defined in (10) only contains polynomials up to order p. Therefore, we have the inclusion

$$\mathbb{T}_p(K) \subset \underline{\boldsymbol{\Sigma}}_h(K). \tag{13}$$

Remark 1. In principle, a lowest order element can be designed as well. In particular, no internal degrees of freedom would be required and slightly different boundary conditions would be imposed in (11); we refer to [5, 17] for more details. The forthcoming analysis generalizes straightforwardly also to this setting, whence we shall skip the details for the presentation's sake.

Degrees of freedom. Hereafter, by scaled polynomial fields we mean polynomial fields $\mathbf{q}_p$ with $\|\mathbf{q}_p\|_{L^\infty(X)} = 1$, $X = K$ or F. Given $\underline{\boldsymbol{\tau}}_h$ in $\mathbb{H}_{\mathcal{S}}(\mathbf{div}, K)$, we consider the following linear functionals:

- for all facets F of K, given a basis $\{\mathbf{m}_{\boldsymbol{\alpha}}^F\}$ of $\mathbf{P}_p(F)$ of scaled polynomial fields that are shifted with respect to $\mathbf{x}_F$, the scaled vector moments of the tractions on F:

$$\frac{1}{|F|}\int_F \underline{\boldsymbol{\tau}}_h \mathbf{n}^K \cdot \mathbf{m}_{\boldsymbol{\alpha}}^F; \tag{14}$$

- given a basis $\{\mathbf{m}_{\boldsymbol{\alpha}}^\perp\}$ of $\mathbf{RM}_p^\perp(K)$ of scaled polynomial fields that are shifted with respect to $\mathbf{x}_K$, the interior scaled vector moments of the divergence:

$$\frac{h_K}{|K|}\int_K \mathbf{div}\,\underline{\boldsymbol{\tau}}_h \cdot \mathbf{m}_{\boldsymbol{\alpha}}^\perp. \tag{15}$$

The above functionals form a set of unisolvent degrees of freedom for $\underline{\boldsymbol{\Sigma}}_h(K)$; see [31, Remark 1].

Polynomial projectors. We introduce several projectors. For each element K, the first one is $\boldsymbol{\Pi}_{\mathbf{RM}} : \mathbf{L}^2(K) \to \mathbf{RM}(K)$ given by

$$(\mathbf{v} - \boldsymbol{\Pi}_{\mathbf{RM}}\mathbf{v}, \mathbf{q}_p^{\mathrm{RM}})_{0,K} = 0 \qquad \forall \mathbf{v} \in \mathbf{L}^2(K),\ \mathbf{q}_p^{\mathrm{RM}} \in \mathbf{RM}(K). \tag{16}$$

Next, we define $\boldsymbol{\Pi}_{\mathbf{RM}}^\perp : \mathbf{L}^2(K) \to \mathbf{RM}^\perp(K)$ as

$$(\mathbf{v} - \boldsymbol{\Pi}_{\mathbf{RM}}^\perp\mathbf{v}, \mathbf{q}_p^\perp)_{0,K} = 0 \qquad \forall \mathbf{v} \in \mathbf{L}^2(K), \quad \mathbf{q}_p^\perp \in \mathbf{RM}^\perp(K). \tag{17}$$

Remark 2. For $\underline{\boldsymbol{\tau}}_h$ in $\underline{\boldsymbol{\Sigma}}_h(K)$, $\boldsymbol{\Pi}_{\mathbf{RM}}\,\mathbf{div}\,\underline{\boldsymbol{\tau}}_h$ can be computed for $\underline{\boldsymbol{\tau}}_h$ in $\underline{\boldsymbol{\Sigma}}_h(K)$ using the boundary degrees of freedom (14); $\boldsymbol{\Pi}_{\mathbf{RM}}^\perp\,\mathbf{div}\,\underline{\boldsymbol{\tau}}_h$ using the interior degrees of freedom (15). Therefore, (9) implies that $\mathbf{div}\,\underline{\boldsymbol{\tau}}_h$ is available in closed-form.

Additionally, we define $\underline{\mathbf{\Pi}}_p^T : \mathbb{L}^2(K) \to \mathbb{T}_p(K)$ as

$$(\mathbb{D}(\underline{\boldsymbol{\tau}} - \underline{\mathbf{\Pi}}_p^T \underline{\boldsymbol{\tau}}), \underline{\mathbf{q}}_p^{\mathbf{T}})_{0,K} = 0 \qquad \forall \underline{\mathbf{q}}_p^{\mathbf{T}} \in \mathbb{T}_p(K). \tag{18}$$

or equivalently

$$(\underline{\boldsymbol{\tau}} - \underline{\mathbf{\Pi}}_p^T \underline{\boldsymbol{\tau}}, \nabla_S(\mathbf{q}_{p+1}))_{0,K} = 0 \qquad \forall \mathbf{q}_{p+1} \in \mathbf{P}_{p+1}(K).$$

The operator $\underline{\mathbf{\Pi}}_p^T$ is computable for functions in $\underline{\mathbf{\Sigma}}_h(K)$ using the degrees of freedom (14) and (15). In fact, as observed for the 2D case in [6, eq. (26)], the orthogonality condition in (18) for $\underline{\boldsymbol{\tau}}$ replaced by $\underline{\boldsymbol{\tau}}_h$ in $\underline{\mathbf{\Sigma}}_h(K)$ is equivalent to find $\underline{\mathbf{r}}_{p+1}$ in $\mathbf{P}_{p+1}(K)$ such that

$$(\mathbb{C}\nabla_S(\underline{\mathbf{r}}_{p+1}), \nabla_S(\mathbf{q}_{p+1}))_{0,K} = (\underline{\boldsymbol{\tau}}_h, \nabla_S(\mathbf{q}_{p+1}))_{0,K} \qquad \forall \mathbf{q}_{p+1} \in \mathbf{P}_{p+1}(K).$$

The right-hand side above is computable via the degrees of freedom (14) and (15) after an integration by parts.

Finally, on each facet F, define $\mathbf{\Pi}_p^{0,F} : \mathbf{L}^2(F) \to \mathbf{P}_p(F)$ as

$$(\mathbf{v} - \mathbf{\Pi}_p^{0,F}\mathbf{v}, \mathbf{q}_p^F)_{0,F} = 0 \qquad \forall \mathbf{v} \in \mathbf{L}^2(F), \qquad \forall \mathbf{q}_p^F \in \mathbf{P}_p(F). \tag{19}$$

Discrete bilinear forms and stabilizations. In the HR virtual element method, the local L^2 inner product $a^K(\underline{\boldsymbol{\sigma}}, \underline{\boldsymbol{\tau}})$ is discretized using two ingredients. The first one is the projector $\underline{\mathbf{\Pi}}_p^T$ in (18); the second one is a bilinear form $S^K(\cdot,\cdot) : \underline{\mathbf{\Sigma}}_h(K) \times \underline{\mathbf{\Sigma}}_h(K) \to \mathbb{R}$ satisfying two properties:

- $S^K(\cdot,\cdot)$ is computable only using the degrees of freedom (14) and (15);
- $S^K(\cdot,\cdot)$ "scales" like $\|\cdot\|_{0,K}^2$ on the kernel of $\underline{\mathbf{\Pi}}_p^T$, i.e., there exist positive constants $\alpha_* \le \alpha^*$ independent of λ, μ, and h_K such that

$$\mu_{|K}^{-1}\alpha_* \|\underline{\boldsymbol{\tau}}_h\|_{0,K}^2 \le S^K(\underline{\boldsymbol{\tau}}_h, \underline{\boldsymbol{\tau}}_h) \le \mu_{|K}^{-1}\alpha^* \|\underline{\boldsymbol{\tau}}_h\|_{0,K}^2 \qquad \forall \underline{\boldsymbol{\tau}}_h \in \underline{\mathbf{\Sigma}}_h(K) \cap \ker(\underline{\mathbf{\Pi}}_p^T). \tag{20}$$

  The constants α_* and α^* may depend on the regularity parameter ρ in Section 1 and p in (11).

Remark 3. For more standard virtual elements (such as those for the approximation of the Poisson problem, the Stokes equations, edge, and face virtual elements ...), the bounds in (20) can be made sharper [28, Corollary 2]: the lower bound is typically proven for functions (fields, tensors, ...) in the virtual element space; the upper bound for functions (fields, tensors, ...) in a Sobolev space with extra zero average conditions. In the HR virtual element setting, this is not possible; see the proof of Proposition 3.2 below.

Let $\mathbb{I}$ be the identity operator. With the two ingredients above at hand, we introduce the local discrete bilinear forms

$$a_h^K(\underline{\boldsymbol{\sigma}}_h, \underline{\boldsymbol{\tau}}_h) := a^K(\underline{\mathbf{\Pi}}_p^T \underline{\boldsymbol{\sigma}}_h, \underline{\mathbf{\Pi}}_p^T \underline{\boldsymbol{\tau}}_h) + S^K((\mathbb{I} - \underline{\mathbf{\Pi}}_p^T)\underline{\boldsymbol{\sigma}}_h, (\mathbb{I} - \underline{\mathbf{\Pi}}_p^T)\underline{\boldsymbol{\tau}}_h) \qquad \forall K \in \mathcal{T}_n. \tag{21}$$

In Section 3 below, we shall exhibit an explicit choice of $S^K(\cdot,\cdot)$ and prove the corresponding stability bounds (20).

3 Explicit stabilizations and stability bounds

We introduce two explicit stabilizations and prove stability bounds as in (20). More precisely, we investigate a "projection-based" stabilization in Section 3.1 and a "dofi-dofi" stabilization in Section 3.2.

3.1 A "projection-based" stabilization

Given $\boldsymbol{\Pi}^{\perp}_{\mathbf{RM}}$ as in (17), for all K in $\mathcal{T}_n$, and all $\underline{\boldsymbol{\sigma}}_h$ and $\underline{\boldsymbol{\tau}}_h$ in $\underline{\boldsymbol{\Sigma}}_h(K)$, we define

$$S^K(\underline{\boldsymbol{\sigma}}_h, \underline{\boldsymbol{\tau}}_h) := \mu_{|K}^{-1} h_K \sum_{F \in \mathcal{F}^K} (\underline{\boldsymbol{\sigma}}_h \mathbf{n}^K, \underline{\boldsymbol{\tau}}_h \mathbf{n}^K)_{0,F} + \mu_{|K}^{-1} h_K^2 (\boldsymbol{\Pi}^{\perp}_{\mathbf{RM}} \mathbf{div}\, \underline{\boldsymbol{\sigma}}_h, \boldsymbol{\Pi}^{\perp}_{\mathbf{RM}} \mathbf{div}\, \underline{\boldsymbol{\tau}}_h)_{0,K}. \quad (22)$$

A practical alternative option discussed in the literature [5, 6] is the stabilization above replacing $\mu_{|K}^{-1}$ by $\mathrm{tr}(\mathbb{D})$.

Proposition 3.1. *The bilinear form $S^K(\cdot,\cdot)$ defined in* (22) *is computable by means of the degrees of freedom* (14) *and* (15)*, and satisfies the stability bounds* (20)*. In fact, the result holds true also for tensors $\underline{\boldsymbol{\tau}}_h$ such that $\underline{\boldsymbol{\Pi}}_p^T \underline{\boldsymbol{\tau}}_h$ is different from the zero tensor.*

Proof. The computability of the bilinear form follows from the computability of $\boldsymbol{\Pi}^{\perp}_{\mathbf{RM}} \mathbf{div}(\cdot)$ for functions in $\underline{\boldsymbol{\Sigma}}_h(K)$, see Remark 2, and the fact that tractions on facets are given polynomials, see (11).

We assume that $h_K = 1$. The general assertion is a consequence of a scaling argument. In what follows, let $\underline{\boldsymbol{\tau}}_h$ solve (11) (or equivalently (12)).

Since the symmetric gradient of a rigid body motion is the zero tensor, we have

$$\nabla_S(\mathbf{div}\, \underline{\boldsymbol{\tau}}_h) = \nabla_S(\boldsymbol{\Pi}^{\perp}_{\mathbf{RM}} \mathbf{div}\, \underline{\boldsymbol{\tau}}_h) \qquad \forall \underline{\boldsymbol{\tau}}_h \in \underline{\boldsymbol{\Sigma}}_h(K). \quad (23)$$

The lower bound. Using Theorem A.7 for the local problem (12) on K, we deduce the existence of a positive constant c_{ST} depending only on ρ in Section 1 such that

$$\|\underline{\boldsymbol{\tau}}_h\|_{0,K} \le \|\underline{\boldsymbol{\tau}}_h\|_{\mathrm{div},K} + \|\mathbf{w}^*\|_{0,K} \le c_{ST} \left(\|\mathbf{div}\, \underline{\boldsymbol{\tau}}_h\|_{0,K} + \left\|\underline{\boldsymbol{\tau}}_h \mathbf{n}^K\right\|_{0,\partial K} \right). \quad (24)$$

Integrating by parts (IBP), and using (23), the Cauchy-Schwarz (CS) inequality, the $H^1 - L^2$ polynomial inverse inequality (II) [30] (constant c^A_{inv}), the fact that $\mathrm{div}\, \underline{\boldsymbol{\tau}}_h$ is a vector polynomial, an inverse L^2 trace inequality (ITI) [30] bounding the L^2 norm on the boundary by the L^2 norm in the interior (constant c^B_{inv}), and two Young's (Y) inequalities with corresponding positive constants ε_1 and ε_2, we write

$$\begin{aligned}
\|\mathbf{div}\, \underline{\boldsymbol{\tau}}_h\|^2_{0,K} &= \int_K \mathbf{div}\, \underline{\boldsymbol{\tau}}_h \cdot \mathbf{div}\, \underline{\boldsymbol{\tau}}_h \overset{\text{(IBP)}}{=} -\int_K \underline{\boldsymbol{\tau}}_h : \nabla_S(\mathbf{div}\, \underline{\boldsymbol{\tau}}_h) + \int_{\partial K} \underline{\boldsymbol{\tau}}_h \mathbf{n}^K \cdot \mathbf{div}\, \underline{\boldsymbol{\tau}}_h \\
&\overset{(23)}{=} -\int_K \underline{\boldsymbol{\tau}}_h : \nabla_S(\boldsymbol{\Pi}^{\perp}_{\mathbf{RM}} \mathbf{div}\, \underline{\boldsymbol{\tau}}_h) + \int_{\partial K} \underline{\boldsymbol{\tau}}_h \mathbf{n}^K \cdot \mathbf{div}\, \underline{\boldsymbol{\tau}}_h \\
&\overset{\text{(CS)}}{\le} \|\underline{\boldsymbol{\tau}}_h\|_{0,K} \left|\boldsymbol{\Pi}^{\perp}_{\mathbf{RM}} \mathbf{div}\, \underline{\boldsymbol{\tau}}_h\right|_{1,K} + \left\|\underline{\boldsymbol{\tau}}_h \mathbf{n}^K\right\|_{0,\partial K} \|\mathbf{div}\, \underline{\boldsymbol{\tau}}_h\|_{0,\partial K} \\
&\overset{\text{(II), (ITI)}}{\le} (c^A_{inv} + c^B_{inv}) \left(\|\underline{\boldsymbol{\tau}}_h\|_{0,K} \left\|\boldsymbol{\Pi}^{\perp}_{\mathbf{RM}} \mathbf{div}\, \underline{\boldsymbol{\tau}}_h\right\|_{0,K} + \left\|\underline{\boldsymbol{\tau}}_h \mathbf{n}^K\right\|_{0,\partial K} \|\mathbf{div}\, \underline{\boldsymbol{\tau}}_h\|_{0,K} \right) \\
&\overset{\text{(Y)}}{=} \frac{1}{2} (c^A_{inv} + c^B_{inv}) \left(\varepsilon_1^2 \|\underline{\boldsymbol{\tau}}_h\|^2_{0,K} + \varepsilon_1^{-2} \left\|\boldsymbol{\Pi}^{\perp}_{\mathbf{RM}} \mathbf{div}\, \underline{\boldsymbol{\tau}}_h\right\|^2_{0,K} + \varepsilon_2^{-2} \left\|\underline{\boldsymbol{\tau}}_h \mathbf{n}^K\right\|^2_{0,\partial K} + \varepsilon_2^2 \|\mathbf{div}\, \underline{\boldsymbol{\tau}}_h\|^2_{0,K} \right).
\end{aligned}$$

Being the constants c^A_{inv} and c^B_{inv} related to polynomial inverse inequalities on (regular subtessellation on) polytopes, they depend on the regularity parameter ρ in Section 1 and p in (11).

Taking ε_2 sufficiently small, we have that there exists a positive c_{ε_2} only depending on ε_2, c^A_{inv}, and c^B_{inv} such that

$$\|\mathbf{div}\, \underline{\boldsymbol{\tau}}_h\|_{0,K} \le c_{\varepsilon_2} \left(\varepsilon_1 \|\underline{\boldsymbol{\tau}}_h\|_{0,K} + \varepsilon_1^{-1} \left\|\boldsymbol{\Pi}^{\perp}_{\mathbf{RM}} \mathbf{div}\, \underline{\boldsymbol{\tau}}_h\right\|_{0,K} + \left\|\underline{\boldsymbol{\tau}}_h \mathbf{n}^K\right\|_{0,\partial K} \right).$$

Inserting this bound in (24) and taking ε_1 sufficiently small yields the assertion: there exists a positive constant c_{ε_1} only depending on ε_1 and c_{ε_2} such that

$$\|\underline{\boldsymbol{\tau}}_h\|_{0,K} \le c_{ST}\ c_{\varepsilon_1} \left(\left\|\underline{\boldsymbol{\tau}}_h \mathbf{n}^K\right\|_{0,\partial K} + \left\|\boldsymbol{\Pi}^{\perp}_{\mathbf{RM}} \mathbf{div}\, \underline{\boldsymbol{\tau}}_h\right\|_{0,K} \right).$$

Notably, the constant α_* in (20) for the stabilization $S^K(\cdot,\cdot)$ in (22) only depends on c^A_{inv}, c^B_{inv}, and c_{ST}.

The upper bound. Using a polynomial inverse inequality [30] on ∂K (constant c_{inv}^C) entails

$$\left\|\underline{\boldsymbol{\tau}}_h\mathbf{n}^K\right\|_{0,\partial K} \leq c_{inv}^C \left\|\underline{\boldsymbol{\tau}}_h\mathbf{n}^K\right\|_{-\frac{1}{2},\partial K}.$$

Being the constant c_{inv}^C related to polynomial inverse inequalities on the boundary of polytopes, it depends on the regularity parameter ρ in Section 1 and p in (11).

Next, we use the $H(\mathrm{div})$ trace inequality (2) (constant c_{tr}) and get

$$\left\|\underline{\boldsymbol{\tau}}_h\mathbf{n}^K\right\|_{-\frac{1}{2},\partial K} \leq c_{tr}\left(\|\underline{\boldsymbol{\tau}}_h\|_{0,K} + \|\mathbf{div}\,\underline{\boldsymbol{\tau}}_h\|_{0,K}\right).$$

It suffices to estimate the second term on the right-hand side. Using the $L^2 - H^{-1}$ polynomial inverse inequality [30] (constant c_{inv}^D), definition (1), an integration by parts, and the Cauchy-Schwarz inequality yields

$$\left\|\boldsymbol{\Pi}^{\perp}_{\mathbf{RM}}\,\mathbf{div}\,\underline{\boldsymbol{\tau}}_h\right\|_{0,K} \leq \|\mathbf{div}\,\underline{\boldsymbol{\tau}}_h\|_{0,K} \leq c_{inv}^D\|\mathbf{div}\,\underline{\boldsymbol{\tau}}_h\|_{-1,K} = c_{inv}^D \sup_{\mathbf{v}\in\mathbf{H}^1_{\mathbf{0}}(K)} \frac{(\mathbf{div}\,\underline{\boldsymbol{\tau}}_h,\mathbf{v})_{0,K}}{|\mathbf{v}|_{1,K}} \leq c_{inv}^D\|\underline{\boldsymbol{\tau}}_h\|_{0,K},$$

thereby implying the upper bound in (20). The constant α^* in (20) for the stabilization $S^K(\cdot,\cdot)$ in (22) only depends on c_{inv}^C, c_{inv}^D, and c_{tr}. □

3.2 A "dofi-dofi" stabilization

With an abuse of notation, we denote the set of the degrees of freedom of $\underline{\mathbf{\Sigma}}_h(K)$ by $\{\mathbf{dof}\}$, which we split into the union of facet $\{\mathbf{dof}^F\}$, for all F facets of K, and the divergence $\{\mathbf{dof}^\perp\}$ degrees of freedom.

Given the standard ℓ^2 inner product $(\cdot,\cdot)_{\ell^2}$ for sequences, we introduce the "dofi-dofi" stabilization $\widetilde{S}^K : \underline{\mathbf{\Sigma}}_h(K)\times\underline{\mathbf{\Sigma}}_h(K)\to\mathbb{R}$ defined on any element K as

$$\begin{aligned}\widetilde{S}^K(\underline{\boldsymbol{\sigma}}_h,\underline{\boldsymbol{\tau}}_h) &:= \mu_{|K}^{-1}h_K^3(\mathbf{dof}(\underline{\boldsymbol{\sigma}}_h),\mathbf{dof}(\underline{\boldsymbol{\tau}}_h))_{\ell^2}\\ &= \mu_{|K}^{-1}h_K^3\sum_{F\in\mathcal{F}^K}(\mathbf{dof}^F(\underline{\boldsymbol{\sigma}}_h),\mathbf{dof}^F(\underline{\boldsymbol{\tau}}_h))_{\ell^2} + \mu_{|K}^{-1}h_K^3(\mathbf{dof}^\perp(\underline{\boldsymbol{\sigma}}_h),\mathbf{dof}^\perp(\underline{\boldsymbol{\tau}}_h))_{\ell^2}.\end{aligned} \tag{25}$$

We prove that this stabilization is equivalent to the "projection based" stabilization in (22) under a suitable choice of the polynomial bases appearing in (14) and (15).

Proposition 3.2. *Given $S^K(\cdot,\cdot)$ and $\widetilde{S}^K(\cdot,\cdot)$ the stabilizations defined in* (22) *and* (25)*, there exist positive constants $\beta_* \leq \beta^*$ such that*

$$\beta_* S^K(\underline{\boldsymbol{\tau}}_h,\underline{\boldsymbol{\tau}}_h) \leq \widetilde{S}^K(\underline{\boldsymbol{\tau}}_h,\underline{\boldsymbol{\tau}}_h) \leq \beta^* S^K(\underline{\boldsymbol{\tau}}_h,\underline{\boldsymbol{\tau}}_h) \qquad \forall\underline{\boldsymbol{\tau}}_h\in\underline{\mathbf{\Sigma}}_h(K),\quad \forall K\in\mathcal{T}_n.$$

The constants β_* and β^* may depend on the regularity parameter ρ in Section 1 and p in (11)*.*

Proof. We show the lower and upper bound separately.

The lower bound (part 1). We first show, for all facets F in $\mathcal{F}^K$, the existence of a positive constant c_1 such that

$$h_K\left\|\underline{\boldsymbol{\tau}}_h\mathbf{n}^K\right\|_{0,F}^2 \leq c_1 h_K^3\left\|\mathbf{dof}^F(\underline{\boldsymbol{\tau}}_h)\right\|_{\ell^2}^2 \qquad \forall\underline{\boldsymbol{\tau}}_h\in\underline{\mathbf{\Sigma}}_h(K). \tag{26}$$

We have the decomposition into polynomial fields on facets

$$\underline{\boldsymbol{\tau}}_h\mathbf{n}^K{}_{|F} = \sum_{|\boldsymbol{\alpha}|=1}^{p}\lambda_{\boldsymbol{\alpha}}^F\mathbf{m}_{\boldsymbol{\alpha}}^F \qquad \text{for given } \lambda_{\boldsymbol{\alpha}}^F\in\mathbb{R}.$$

Testing both sides by $\mathbf{m}_{\boldsymbol{\beta}}^F$, scaling by the area of the facet F, and using that the $\underline{\boldsymbol{\tau}}_h\mathbf{n}^K$ are linear combinations of scaled orthogonal polynomial fields, we deduce

$$\mathbf{dof}_{\boldsymbol{\beta}}^F(\underline{\boldsymbol{\tau}}_h) = \frac{1}{|F|}\int_F(\underline{\boldsymbol{\tau}}_h\mathbf{n}^K)\cdot\mathbf{m}_{\boldsymbol{\beta}}^F = \frac{1}{|F|}\sum_{|\boldsymbol{\alpha}|=0}^{p}\lambda_{\boldsymbol{\alpha}}^F\int_F\mathbf{m}_{\boldsymbol{\alpha}}^F\cdot\mathbf{m}_{\boldsymbol{\beta}}^F. \tag{27}$$

Collect the coefficients $\lambda^F_{\boldsymbol{\alpha}}$ in a vector $\boldsymbol{\lambda}^F$. Using the arguments as in [12, Lemma 4.1], there exists a positive constant c^A_{CH}, which only depends on ρ in Section 1 and p in (11), such that

$$\left\|\underline{\boldsymbol{\tau}}_h\mathbf{n}^K\right\|^2_{0,F} \leq c^A_{CH}h_K^2\left\|\boldsymbol{\lambda}^F\right\|^2_{\ell^2}.$$

Further using (27), we deduce (26).

The lower bound (part 2). We prove that there exists a positive constant c_2 such that

$$h_K^2(\boldsymbol{\Pi}^\perp_{\mathbf{RM}}\operatorname{\mathbf{div}}\underline{\boldsymbol{\sigma}}_h, \boldsymbol{\Pi}^\perp_{\mathbf{RM}}\operatorname{\mathbf{div}}\underline{\boldsymbol{\tau}}_h)_{0,K} \leq c_2h_K^3(\mathbf{dof}^\perp(\underline{\boldsymbol{\sigma}}_h), \mathbf{dof}^\perp(\underline{\boldsymbol{\tau}}_h))_{\ell^2}. \tag{28}$$

We have the decomposition into polynomial fields, which are orthogonal to rigid body motions,

$$\boldsymbol{\Pi}^\perp_{\mathbf{RM}}\operatorname{\mathbf{div}}\underline{\boldsymbol{\tau}}_h = \sum_{|\boldsymbol{\alpha}|=0}^{p}\mu^\perp_{\boldsymbol{\alpha}}\mathbf{m}^\perp_{\boldsymbol{\alpha}} \qquad \text{for given } \mu^\perp_{\boldsymbol{\alpha}} \in \mathbb{R}.$$

Testing on both sides by $\mathbf{m}^\perp_{\boldsymbol{\beta}}$ and using that the $\mathbf{m}^\perp_{\boldsymbol{\alpha}}$ are linear combinations of scaled orthogonal polynomial fields, we deduce

$$\mathbf{dof}^\perp_{\boldsymbol{\beta}}(\underline{\boldsymbol{\tau}}_h) = \frac{h_K}{|K|}\int_K \operatorname{\mathbf{div}}\underline{\boldsymbol{\tau}}_h\cdot\mathbf{m}^\perp_{\boldsymbol{\beta}} = \sum_{|\boldsymbol{\alpha}|=1}^{p}\mu^\perp_{\boldsymbol{\alpha}}\frac{h_K}{|K|}\int_K \mathbf{m}^\perp_{\boldsymbol{\alpha}}\cdot\mathbf{m}^\perp_{\boldsymbol{\beta}}. \tag{29}$$

Collect the coefficients $\mu^\perp_{\boldsymbol{\alpha}}$ in a vector $\boldsymbol{\mu}^\perp$. Using the arguments for the 3D version of [12, Lemma 4.1], there exists a positive constant c^B_{CH}, which only depends on ρ in Section 1 and p in (11), such that

$$\left\|\boldsymbol{\Pi}^\perp_{\mathbf{RM}}\operatorname{\mathbf{div}}\underline{\boldsymbol{\tau}}_h\right\|^2_{0,K} \leq c^B_{CH}h_K^3\left\|\boldsymbol{\mu}^\perp\right\|^2_{\ell^2} = c^B_{CH}h_K\left\|h_K\boldsymbol{\mu}^\perp\right\|^2_{\ell^2}.$$

Further using (29), we deduce (28).

Combining bounds (26) and (28) yields the lower bound.

The upper bound (part 1). We show, for all facets F in $\mathcal{F}^K$, the existence of a positive constant c_3 such that

$$h_K^3\left\|\mathbf{dof}^F(\underline{\boldsymbol{\tau}}_h)\right\|^2_{\ell^2} \leq c_3h_K\left\|\underline{\boldsymbol{\tau}}_h\mathbf{n}^K\right\|^2_{0,F} \qquad \forall\underline{\boldsymbol{\tau}}_h \in \underline{\boldsymbol{\Sigma}}_h(K). \tag{30}$$

Since $\left\|\mathbf{m}^F_{\boldsymbol{\beta}}\right\|_{L^\infty(F)} = 1$, we have

$$\mathbf{dof}^F_{\boldsymbol{\beta}}(\underline{\boldsymbol{\tau}}_h) = \frac{1}{|F|}\int_F \underline{\boldsymbol{\tau}}_h\mathbf{n}^K\cdot\mathbf{m}^F_{\boldsymbol{\beta}} \leq \frac{1}{|F|^{\frac{1}{2}}}\left\|\underline{\boldsymbol{\tau}}_h\mathbf{n}^K\right\|_{0,F} \leq C_\rho h_K^{-1}\left\|\underline{\boldsymbol{\tau}}_h\mathbf{n}^K\right\|_{0,F},$$

for some positive constant C_ρ only depending on ρ in Section 1.

This gives

$$h_K^3\,\mathbf{dof}^F_{\boldsymbol{\beta}}(\underline{\boldsymbol{\tau}}_h)^2 \leq C_\rho^2h_K\left\|\underline{\boldsymbol{\tau}}_h\mathbf{n}^K\right\|^2_{0,F}.$$

Summing over the correct multi-indices gives (30) for all facets F of K.

The upper bound (part 2). We prove the existence of a positive constant c_4 such that

$$h_K^3(\mathbf{dof}^\perp(\underline{\boldsymbol{\sigma}}_h), \mathbf{dof}^\perp(\underline{\boldsymbol{\tau}}_h))_{\ell^2} \leq c_4h_K^2(\boldsymbol{\Pi}^\perp_{\mathbf{RM}}\operatorname{\mathbf{div}}\underline{\boldsymbol{\sigma}}_h, \boldsymbol{\Pi}^\perp_{\mathbf{RM}}\operatorname{\mathbf{div}}\underline{\boldsymbol{\tau}}_h)_{0,K}. \tag{31}$$

Since $\left\|\mathbf{m}^\perp_{\boldsymbol{\beta}}\right\|_{L^\infty(K)} = 1$, we have

$$\mathbf{dof}^\perp_{\boldsymbol{\beta}}(\underline{\boldsymbol{\tau}}_h) = \frac{h_K}{|K|}\int_K \operatorname{\mathbf{div}}\underline{\boldsymbol{\tau}}_h\mathbf{m}^\perp_{\boldsymbol{\beta}} \leq \frac{h_K}{|K|^{\frac{1}{2}}}\left\|\boldsymbol{\Pi}^\perp_{\mathbf{RM}}\operatorname{\mathbf{div}}\underline{\boldsymbol{\tau}}_h\right\|_{0,K} \leq C_\rho h_K^{-\frac{1}{2}}\left\|\boldsymbol{\Pi}^\perp_{\mathbf{RM}}\operatorname{\mathbf{div}}\underline{\boldsymbol{\tau}}_h\right\|_{0,K},$$

for some positive constant C_ρ only depending on ρ in Section 1.

This yields

$$h_K^3 \, \mathbf{dof}_{\boldsymbol{\beta}}^{\perp}(\underline{\boldsymbol{\tau}}_h)^2 \leq C_\rho^2 h_K^2 \left\| \boldsymbol{\Pi}_{\mathbf{RM}}^{\perp} \mathbf{div}\, \underline{\boldsymbol{\tau}}_h \right\|_{0,F}^2.$$

Summing over the correct multi-indices gives (31). □

An immediate consequence of Propositions 3.1 and 3.2 is the following result.

Corollary 3.3. *The bilinear form $\widetilde{S}^K(\cdot,\cdot)$ defined in (25) satisfies the stability bounds (20). In fact, the result holds true also for tensors $\underline{\boldsymbol{\tau}}_h$ such that $\underline{\boldsymbol{\Pi}}_p^T \underline{\boldsymbol{\tau}}_h$ is different from the zero tensor.*

Remark 4. In the virtual element discretization of (6), displacements are vector, piecewise polynomials of degree p; see [6, 31]. In particular, $\operatorname{div} \underline{\boldsymbol{\Sigma}}_h(K)$ coincides with that space and therefore the discrete stress solution is also the solution to the reduced problem on the discrete kernel of the mixed method. Based on this, the stability bounds (20) should be valid for divergence free discrete tensors in $\underline{\boldsymbol{\tau}}_h$ in $\underline{\boldsymbol{\Sigma}}_h(K) \cap \ker(\underline{\boldsymbol{\Pi}}_p^T)$. Reduced versions of the bilinear forms $S^K(\cdot,\cdot)$ and $\widetilde{S}^K(\cdot,\cdot)$ may be employed: in the former case, the divergence term vanishes; in the latter, only facet degrees of freedom are employed (this is in fact the original stabilization proposed in [6, 31]). On the theoretical level, we have the following advantages: no polynomial inverse inequalities are needed in the proof of the lower bound in Proposition 3.1; in the proof of Proposition 3.2, the "parts 2" can be skipped.

4 Interpolation estimates

We derive interpolation estimates for functions in HR virtual element spaces based on the stability bounds derived in Proposition 3.1. Related but different interpolation results can be found in [5, Proposition 5.3], [6, Proposition 4.2], [17, Proposition 4.2], and [31, Proposition 4.4].

Given an element K and a sufficiently smooth (in the sense of Remark 5 below) stress $\underline{\boldsymbol{\sigma}}$, we consider the unique discrete stress $\underline{\boldsymbol{\sigma}}_I$ in $\underline{\boldsymbol{\Sigma}}_h$ sharing the degrees of freedom of $\underline{\boldsymbol{\sigma}}$. More precisely, we define $\underline{\boldsymbol{\sigma}}_I$ as the only function in $\underline{\boldsymbol{\Sigma}}_h$ satisfying

$$\begin{aligned} \int_K \mathbf{div}(\underline{\boldsymbol{\sigma}} - \underline{\boldsymbol{\sigma}}_I) \cdot \mathbf{q}_p^{\perp} &= 0 \qquad && \forall \mathbf{q}_p^{\perp} \in \mathbf{RM}^{\perp}(K),\ \forall K \in \mathcal{T}_n, \\ \int_F (\underline{\boldsymbol{\sigma}} - \underline{\boldsymbol{\sigma}}_I)\mathbf{n}^K \cdot \mathbf{q}_p^F &= 0 \qquad && \forall \mathbf{q}_p^F \in \mathbf{P}_p(F),\ \forall F \in \mathcal{F}^K,\ \forall K \in \mathcal{T}_n. \end{aligned} \tag{32}$$

Remark 5. We need sufficient regularity for the stress $\underline{\boldsymbol{\sigma}}$ in order to define its interpolant $\underline{\boldsymbol{\sigma}}_I$ in the sense of (32). For instance, if $\underline{\boldsymbol{\sigma}}$ belongs to $\mathbb{H}_S(\mathbf{div},\Omega) \cap \mathbb{H}^{\frac{1}{2}+\varepsilon}(\Omega)$, $\varepsilon > 0$, $\mathbf{div}\,\underline{\boldsymbol{\sigma}}$ belongs to $\mathbf{L}^2(\Omega)$ and $\underline{\boldsymbol{\sigma}}\mathbf{n}^K{}_{|F}$ belongs to $\mathbf{L}^2(F)$ for all facets F in the mesh, whence the integrals in (32) are well defined. Lower regularity can be demanded following, e.g., [10, eq. (2.5.1)] or [20, Sect. 17.2]: it suffices that $\underline{\boldsymbol{\sigma}}$ belongs to the space of symmetric stresses with $\underline{\boldsymbol{\sigma}}$ in $\mathbb{L}^s(\Omega)$, $s > 2$, and $\mathbf{div}\,\underline{\boldsymbol{\sigma}}$ in $\mathbf{L}^q(\Omega)$, $q > 6/5$. In this case, the integrals in (32) make sense up to face-to-cell liftings.

For $\boldsymbol{\Pi}_{\mathbf{RM}}^{\perp}$ and $\boldsymbol{\Pi}_p^{0,F}$ as in (17) and (19), and sufficiently smooth stresses, definition (32) gives

$$\boldsymbol{\Pi}_{\mathbf{RM}}^{\perp} \mathbf{div}\, \underline{\boldsymbol{\sigma}}_I = \boldsymbol{\Pi}_{\mathbf{RM}}^{\perp} \mathbf{div}\, \underline{\boldsymbol{\sigma}}, \qquad (\underline{\boldsymbol{\sigma}}_I \mathbf{n}^K)_{|F} = \boldsymbol{\Pi}_p^{0,F}(\underline{\boldsymbol{\sigma}}\mathbf{n}^K)_{|F} \quad \forall F \in \mathcal{F}^K. \tag{33}$$

We have the following commutative property.

Lemma 4.1. *Given $\underline{\boldsymbol{\sigma}}$ satisfying one of the two assumptions in Remark 5 and $\underline{\boldsymbol{\sigma}}_I$ its interpolant in $\underline{\boldsymbol{\Sigma}}_h$ as in (32), we have the following identity:*

$$(\mathbf{div}\, \underline{\boldsymbol{\sigma}}_I)_{|K} = \boldsymbol{\Pi}_p^{0,K}(\mathbf{div}\, \underline{\boldsymbol{\sigma}})_{|K} \qquad \forall K \in \mathcal{T}_n. \tag{34}$$

Proof. The proof is based on the arguments in Remark 2. The divergence of functions in $\underline{\boldsymbol{\Sigma}}_h(K)$ is a polynomial field. Given $\boldsymbol{\Pi}_{\mathbf{RM}}$ and $\boldsymbol{\Pi}_{\mathbf{RM}}^{\perp}$ as in (16) and (17), we recall the orthogonal splitting

$$(\mathbf{div}\, \underline{\boldsymbol{\sigma}}_I)_{|K} = \boldsymbol{\Pi}_{\mathbf{RM}}(\mathbf{div}\, \underline{\boldsymbol{\sigma}}_I)_{|K} + \boldsymbol{\Pi}_{\mathbf{RM}}^{\perp}(\mathbf{div}\, \underline{\boldsymbol{\sigma}}_I)_{|K} \qquad \forall K \in \mathcal{T}_n. \tag{35}$$

Using the first condition in (32), we write

$$\int_K \mathbf{\Pi}^{\perp}_{\mathbf{RM}} \mathbf{div}\, \underline{\boldsymbol{\sigma}}_I \cdot \mathbf{q}_p^{\perp} = \int_K \mathbf{div}\, \underline{\boldsymbol{\sigma}}_I \cdot \mathbf{q}_p^{\perp} = \int_K \mathbf{div}\, \underline{\boldsymbol{\sigma}} \cdot \mathbf{q}_p^{\perp} = \int_K \mathbf{\Pi}^{\perp}_{\mathbf{RM}} \mathbf{div}\, \underline{\boldsymbol{\sigma}} \cdot \mathbf{q}_p^{\perp} \quad \forall \mathbf{q}_p^{\perp} \in \mathbf{RM}^{\perp}(K).$$

This implies that

$$\mathbf{\Pi}^{\perp}_{\mathbf{RM}}(\mathbf{div}\, \underline{\boldsymbol{\sigma}}_I)_{|K} = \mathbf{\Pi}^{\perp}_{\mathbf{RM}}(\mathbf{div}\, \underline{\boldsymbol{\sigma}})_{|K} \qquad \forall K \in \mathcal{T}_n.$$

On the other hand, integrating by parts, using the second condition in (32), and exploiting the fact that $\nabla_S(\mathbf{q}_p^{\mathrm{RM}})$ is zero for all rigid body motions $\mathbf{q}_p^{\mathrm{RM}}$, we also deduce [1]

$$\int_K \mathbf{\Pi}_{\mathbf{RM}} \mathbf{div}\, \underline{\boldsymbol{\sigma}}_I \cdot \mathbf{q}_p^{\mathrm{RM}} = \int_K \mathbf{div}\, \underline{\boldsymbol{\sigma}}_I \cdot \mathbf{q}_p^{\mathrm{RM}} = -\int_K \underline{\boldsymbol{\sigma}}_I : \nabla_S(\mathbf{q}_p^{\mathrm{RM}}) + \sum_{F \in \mathcal{F}^K} \int_F \underline{\boldsymbol{\sigma}}_I \mathbf{n}^K \cdot \mathbf{q}_p^{\mathrm{RM}}$$
$$= -\int_K \underline{\boldsymbol{\sigma}} : \nabla_S(\mathbf{q}_p^{\mathrm{RM}}) + \sum_{F \in \mathcal{F}^K} \int_F \underline{\boldsymbol{\sigma}} \mathbf{n}^K \cdot \mathbf{q}_p^{\mathrm{RM}} = \int_K \mathbf{div}\, \underline{\boldsymbol{\sigma}} \cdot \mathbf{q}_p^{\mathrm{RM}} = \int_K \mathbf{\Pi}_{\mathbf{RM}} \mathbf{div}\, \underline{\boldsymbol{\sigma}} \cdot \mathbf{q}_p^{\mathrm{RM}}.$$

This implies that

$$\mathbf{\Pi}_{\mathbf{RM}}(\mathbf{div}\, \underline{\boldsymbol{\sigma}}_I)_{|K} = \mathbf{\Pi}_{\mathbf{RM}}(\mathbf{div}\, \underline{\boldsymbol{\sigma}})_{|K} \qquad \forall K \in \mathcal{T}_n.$$

Inserting the displays above in (35) and recalling the orthogonal decomposition (9), we obtain

$$(\mathbf{div}\, \underline{\boldsymbol{\sigma}}_I)_{|K} = \mathbf{\Pi}_{\mathbf{RM}}(\mathbf{div}\, \underline{\boldsymbol{\sigma}})_{|K} + \mathbf{\Pi}^{\perp}_{\mathbf{RM}}(\mathbf{div}\, \underline{\boldsymbol{\sigma}})_{|K} = \mathbf{\Pi}_p^{0,K}(\mathbf{div}\, \underline{\boldsymbol{\sigma}})_{|K} \qquad \forall K \in \mathcal{T}_n.$$

□

Introduce the local spaces

$$\widetilde{\underline{\mathbf{\Sigma}}}(K) := \{\underline{\boldsymbol{\tau}} \in \mathbb{H}_{\mathcal{S}}(\mathbf{div}, K) \mid \exists\, \mathbf{w} \in \mathbf{H}^1(K) \text{ such that } \underline{\boldsymbol{\tau}} = \mathbb{C}\nabla_S(\mathbf{w})\} \qquad \forall K \in \mathcal{T}_n.$$

The following polynomial approximation result is valid; see [6, Proposition 3.2] and [31, Proposition 4.3].

Lemma 4.2. *Let $\underline{\boldsymbol{\sigma}}$ belong to $\widetilde{\underline{\mathbf{\Sigma}}}(K) \cap \mathbb{H}^r(K)$, r nonnegative, and r be smaller than or equal to $p+1$. Given $\underline{\mathbf{\Pi}}_p^T$ as in* (18)*, the following bound holds true: there exists a positive constant C only depending on the regularity parameter ρ in Section 1 and p in* (11) *such that*

$$\left\| \underline{\boldsymbol{\sigma}} - \underline{\mathbf{\Pi}}_p^T \underline{\boldsymbol{\sigma}} \right\|_{0,K} \le C h_K^r |\underline{\boldsymbol{\sigma}}|_{r,K}.$$

We are now in a position to prove interpolation estimates in HR virtual element spaces in the L^2 norm and in the L^2 norm of the divergence.

Theorem 4.3. *If $\underline{\boldsymbol{\sigma}}$ belongs to $\widetilde{\underline{\mathbf{\Sigma}}}(K) \cap \mathbb{H}^r(K)$, $r > 1/2 + \varepsilon$ for some $\varepsilon > 0$, and r is smaller than or equal to $p+1$, then there exists a positive constant c depending only on the shape of K and p in* (11) *such that*

$$\|\underline{\boldsymbol{\sigma}} - \underline{\boldsymbol{\sigma}}_I\|_{0,K} \le c h_K^r |\underline{\boldsymbol{\sigma}}|_{r,K} \qquad \forall K \in \mathcal{T}_n. \tag{36}$$

If $\underline{\boldsymbol{\sigma}}$ belongs to $\widetilde{\underline{\mathbf{\Sigma}}}(K) \cap \mathbb{L}^s(\Omega)$, $s > 2$, and $\mathbf{div}\, \underline{\boldsymbol{\sigma}}$ in $\mathbf{H}^t(\Omega)$, $t \ge 0$, and t is smaller than or equal to $p+1$, then there exists a positive constant c depending only on the shape of K and p in (11) *such that*

$$\|\mathrm{div}(\underline{\boldsymbol{\sigma}} - \underline{\boldsymbol{\sigma}}_I)\|_{0,K} \le c h_K^t |\mathbf{div}\, \underline{\boldsymbol{\sigma}}|_{t,K} \qquad \forall K \in \mathcal{T}_n. \tag{37}$$

Proof. Bound (37) follows from (34) and polynomial approximation properties. In particular, the constant c is that of a best polynomial approximation result.

As for bound (36), we first observe that (13) entails $\underline{\mathbf{q}}_p^{\mathbf{T}} = (\underline{\mathbf{q}}_p^{\mathbf{T}})_I$ for any given $\underline{\mathbf{q}}_p^{\mathbf{T}}$ in $\mathbb{T}_p(K)$. Next, we apply the triangle inequality and the lower bound as in Proposition 3.1 to get, for all $\underline{\mathbf{q}}_p^{\mathbf{T}}$ in $\mathbb{T}_p(K)$,

$$\|\underline{\boldsymbol{\sigma}} - \underline{\boldsymbol{\sigma}}_I\|_{0,K} \le \left\| \underline{\boldsymbol{\sigma}} - \underline{\mathbf{q}}_p^{\mathbf{T}} \right\|_{0,K} + \left\| (\underline{\boldsymbol{\sigma}} - \underline{\mathbf{q}}_p^{\mathbf{T}})_I \right\|_{0,K} \le \left\| \underline{\boldsymbol{\sigma}} - \underline{\mathbf{q}}_p^{\mathbf{T}} \right\|_{0,K} + \alpha_*^{-1} \mu_{|K} S^K((\underline{\boldsymbol{\sigma}} - \underline{\mathbf{q}}_p^{\mathbf{T}})_I, (\underline{\boldsymbol{\sigma}} - \underline{\mathbf{q}}_p^{\mathbf{T}})_I).$$

[1] The L^2 inner products on facets should be replaced by suitable duality pairings in case $\underline{\boldsymbol{\sigma}}$ satisfies the second regularity assumption in Remark 5.

Since the first term on the right-hand side yields optimal error estimates, see Lemma 4.2, with constant that only depends on the regularity parameter ρ in Section 1 and p in (11), we only focus on the second one.

Putting aside the parameter α_*^{-1}, and recalling (22) and (33), we write

$$\begin{aligned}\mu_{|K} S^K((\underline{\boldsymbol{\sigma}} - \underline{\mathbf{q}}_p^{\mathbf{T}})_I, (\underline{\boldsymbol{\sigma}} - \underline{\mathbf{q}}_p^{\mathbf{T}})_I) &= h_K \sum_{F \in \mathcal{F}^K} \left\| (\underline{\boldsymbol{\sigma}} - \underline{\mathbf{q}}_p^{\mathbf{T}})_I \mathbf{n}^K \right\|_{0,F}^2 + h_K^2 \left\| \boldsymbol{\Pi}^{\perp}_{\mathbf{RM}} \mathbf{div}(\underline{\boldsymbol{\sigma}} - \underline{\mathbf{q}}_p^{\mathbf{T}})_I \right\|_{0,K}^2 \\ &= h_K \sum_{F \in \mathcal{F}^K} \left\| \boldsymbol{\Pi}_p^{0,F}((\underline{\boldsymbol{\sigma}} - \underline{\mathbf{q}}_p^{\mathbf{T}})\mathbf{n}^K) \right\|_{0,F}^2 + h_K^2 \left\| \boldsymbol{\Pi}^{\perp}_{\mathbf{RM}} \mathbf{div}(\underline{\boldsymbol{\sigma}} - \underline{\mathbf{q}}_p^{\mathbf{T}}) \right\|_{0,K}^2.\end{aligned}$$

As for the first term on the right-hand side, for each facet F, we use the stability of the L^2 projector on facets, the trace [20, Theorem 3.10] and the Poincaré inequality [20, Section 3.3], the triangle inequality, a polynomial inverse inequality [30], and get, for a suitable polynomial approximant $\underline{\mathbf{q}}_p$ of $\underline{\boldsymbol{\sigma}}$, e.g., the tensor Bramble-Hilbert polynomial,

$$\begin{aligned}&h_K \left\| \boldsymbol{\Pi}_p^{0,F}((\underline{\boldsymbol{\sigma}} - \underline{\mathbf{q}}_p^{\mathbf{T}})\mathbf{n}^K) \right\|_{0,F}^2 \leq h_K \left\| \underline{\boldsymbol{\sigma}} - \underline{\mathbf{q}}_p^{\mathbf{T}} \right\|_{0,F}^2 \lesssim h_K^{1+2\varepsilon} \left| \underline{\boldsymbol{\sigma}} - \underline{\mathbf{q}}_p^{\mathbf{T}} \right|_{\frac{1}{2}+\varepsilon,K}^2 \\ &\lesssim h_K^{1+2\varepsilon} \left(\left| \underline{\boldsymbol{\sigma}} - \underline{\mathbf{q}}_p \right|_{\frac{1}{2}+\varepsilon,K}^2 + \left| \underline{\mathbf{q}}_p - \underline{\mathbf{q}}_p^{\mathbf{T}} \right|_{\frac{1}{2}+\varepsilon,K}^2 \right) \lesssim h_K^{1+2\varepsilon} \left| \underline{\boldsymbol{\sigma}} - \underline{\mathbf{q}}_p \right|_{\frac{1}{2}+\varepsilon,K}^2 + \left\| \underline{\mathbf{q}}_p - \underline{\mathbf{q}}_p^{\mathbf{T}} \right\|_{0,K}^2 \qquad (38) \\ &\lesssim h_K^{1+2\varepsilon} \left| \underline{\boldsymbol{\sigma}} - \underline{\mathbf{q}}_p \right|_{\frac{1}{2}+\varepsilon,K}^2 + \left\| \underline{\boldsymbol{\sigma}} - \underline{\mathbf{q}}_p^{\mathbf{T}} \right\|_{0,K}^2.\end{aligned}$$

The hidden constants depend on ρ in Section 1 and p in (11). The above inequality gives

$$\begin{aligned}S^K((\underline{\boldsymbol{\sigma}} - \underline{\mathbf{q}}_p^{\mathbf{T}})_I, (\underline{\boldsymbol{\sigma}} - \underline{\mathbf{q}}_p^{\mathbf{T}})_I) &\lesssim h_K^{1+2\varepsilon} \left| \underline{\boldsymbol{\sigma}} - \underline{\mathbf{q}}_p \right|_{\frac{1}{2}+\varepsilon,K}^2 + \left\| \underline{\boldsymbol{\sigma}} - \underline{\mathbf{q}}_p^{\mathbf{T}} \right\|_{0,K}^2 + h_K^2 \left\| \boldsymbol{\Pi}^{\perp}_{\mathbf{RM}} \mathbf{div}(\underline{\boldsymbol{\sigma}} - \underline{\mathbf{q}}_p^{\mathbf{T}}) \right\|_{0,K}^2 \\ &\leq h_K^{1+2\varepsilon} \left| \underline{\boldsymbol{\sigma}} - \underline{\mathbf{q}}_p \right|_{\frac{1}{2}+\varepsilon,K}^2 + \left\| \underline{\boldsymbol{\sigma}} - \underline{\mathbf{q}}_p^{\mathbf{T}} \right\|_{0,K}^2 + h_K^2 \left\| \mathbf{div}(\underline{\boldsymbol{\sigma}} - \underline{\mathbf{q}}_p^{\mathbf{T}}) \right\|_{0,K}^2.\end{aligned}$$

The first two terms on the right-hand side converge optimally due to polynomial approximation estimates and Lemma 4.2; thence, we focus on the second one. Proceeding as in (38) leads us to

$$\begin{aligned}\left\| \mathbf{div}(\underline{\boldsymbol{\sigma}} - \underline{\mathbf{q}}_p^{\mathbf{T}}) \right\|_{0,K} &\leq \left\| \mathbf{div}(\underline{\boldsymbol{\sigma}} - \underline{\mathbf{q}}_p) \right\|_{0,K} + \left\| \mathbf{div}(\underline{\mathbf{q}}_p - \underline{\mathbf{q}}_p^{\mathbf{T}}) \right\|_{0,K} \\ &\lesssim \left\| \mathbf{div}(\underline{\boldsymbol{\sigma}} - \underline{\mathbf{q}}_p) \right\|_{0,K} + h_K^{-1} \left\| \underline{\mathbf{q}}_p - \underline{\mathbf{q}}_p^{\mathbf{T}} \right\|_{0,K} \\ &\leq \left\| \mathbf{div}(\underline{\boldsymbol{\sigma}} - \underline{\mathbf{q}}_p) \right\|_{0,K} + h_K^{-1} \left\| \underline{\boldsymbol{\sigma}} - \underline{\mathbf{q}}_p \right\|_{0,K} + h_K^{-1} \left\| \underline{\boldsymbol{\sigma}} - \underline{\mathbf{q}}_p^{\mathbf{T}} \right\|_{0,K}.\end{aligned}$$

Polynomial approximation estimates and Lemma 4.2 yield the assertion. □

Remark 6. Bound (37) can be weakened by taking the $\mathbf{L}^q(K)$ norm of $\mathbf{div}(\underline{\boldsymbol{\sigma}} - \underline{\boldsymbol{\sigma}}_I)$ and the (Banach) Sobolev $\mathbf{W}^{t,q}(K)$ seminorm of $\mathbf{div}\,\underline{\boldsymbol{\sigma}}$, $t > 0$, $q > 6/5$, t smaller than or equal to $p+1$, on the left- and right-hand sides, respectively, in case $\underline{\boldsymbol{\sigma}}$ satisfies the second regularity assumption in Remark 5.

5 A numerical investigation on the stability constants

In this section, we discuss a practical approximation of the coercivity and continuity constants of the discrete bilinear forms in (21), see Section 5.1, and assess numerically their behaviour on sequences of elements with increasing aspect ratio, see Section 5.2, and with increasing degree of accuracy on fixed elements, see Section 5.3. We shall also be focusing on 2D elements. The implementation is based on the C++ library Vem++ [16].

5.1 Computation of the coercivity and continuity constants

Given an element K and the dimension N_{dof}^K of the space $\underline{\boldsymbol{\Sigma}}_h(K)$, let $\{\underline{\boldsymbol{\varphi}}_i\}_{i=1}^{N_{dof}^K}$ be the basis of $\underline{\boldsymbol{\Sigma}}_h(K)$ dual to the degrees of freedom in (14) and (15). Define the symmetric matrices $\mathbf{A}$ and $\mathbf{B}$

$$\mathbf{A}_{i,j} := a_h^K(\underline{\boldsymbol{\varphi}}_j, \underline{\boldsymbol{\varphi}}_i), \qquad \mathbf{B}_{i,j} := (\mathbb{D}\underline{\boldsymbol{\varphi}}_j, \underline{\boldsymbol{\varphi}}_i)_{0,K} \qquad \forall i,j = 1, \ldots, N_{dof}^K. \qquad (39)$$

In this section, we discuss a practical approximation of the coercivity and continuity constants of the discrete bilinear forms $a_h^K(\cdot,\cdot)$ in (21). It can be readily seen that these constants are the minimum and maximum eigenvalues of the following generalized eigenvalue problem: find the eigenpair $(\beth, \mathbf{v})$ satisfying

$$\mathbf{A}\mathbf{v} = \beth \mathbf{B}\mathbf{v}. \tag{40}$$

We recall that the bilinear forms $a_h^K(\cdot,\cdot)$ are computable via the degrees of freedom: it suffices to compute the projector $\underline{\mathbf{\Pi}}_p^T$ in (18) and the stabilization. Therefore, the computation of the matrix $\mathbf{A}$ in (39) is rather simple.

Instead, the computation of the matrix $\mathbf{B}$ is less immediate: the virtual element basis tensors are not available in closed form; as such, they need to be approximated. To this aim, we proceed in several steps.

Step 1. We partition the set of local basis tensors into basis tensors dual to facet (14) and bulk (15) moments:

$$\left\{\underline{\boldsymbol{\varphi}}^B\right\}, \qquad\qquad \left\{\underline{\boldsymbol{\varphi}}^\perp\right\}.$$

According to (11), a basis function $\underline{\boldsymbol{\varphi}}^B$ dual to (14) and associated with a facet F satisfies

$$\mathbf{div}\,\underline{\boldsymbol{\varphi}}^B = \mathbf{r} \in \mathbf{RM}(K), \qquad \underline{\boldsymbol{\varphi}}^B \mathbf{n}^K{}_{|F} = \mathbf{q}_p^F \in \mathbf{P}_p(F), \qquad \underline{\boldsymbol{\varphi}}^B \mathbf{n}^K{}_{|\partial K \setminus F} = \mathbf{0}; \tag{41}$$

a bulk basis function $\underline{\boldsymbol{\varphi}}^K$ dual to (15) satisfies

$$\mathbf{div}\,\underline{\boldsymbol{\varphi}}^\perp = \mathbf{r}_p^\perp \in \mathbf{RM}^\perp(K), \qquad \underline{\boldsymbol{\varphi}}^B\ \mathbf{n}^K{}_{|\partial K} = \mathbf{0}. \tag{42}$$

In (41), $\mathbf{r}$ is constructed using only $\mathbf{q}_p^F$; see also Remark 2. In particular, compatibility conditions are valid through the divergence theorem.

Step 2. We define displacements $\{\mathbf{z}_i\}_{i=1}^{N_{dof}^K}$ such that we have

$$(\mathbb{D}\underline{\boldsymbol{\varphi}}_j, \underline{\boldsymbol{\varphi}}_i)_{0,K} = (\mathbb{C}\nabla_S \mathbf{z}_j, \nabla_S \mathbf{z}_i)_{0,K} \qquad \forall i,j = 1,\dots,N_{dof}^K. \tag{43}$$

A concrete realization of such displacements is given by the solutions to "face–type"

$$\begin{cases} -\mathbf{div}(\mathbb{C}\nabla_S(\mathbf{z}_i^B)) \overset{(41)}{=} -\mathbf{r}_i & \text{in } K \\ \mathbb{C}\nabla_S(\mathbf{z}_i^B)\mathbf{n} \overset{(41)}{=} \mathbf{q}_{p,i}^F & \text{on } F \\ \mathbb{C}\nabla_S(\mathbf{z}_i^B)\mathbf{n} \overset{(41)}{=} \mathbf{0} & \text{on } \partial K \setminus F \end{cases} \tag{44}$$

with $\mathbf{r}_i$ satisfying a compatibility condition with the Neumann boundary condition, and "bulk–type"

$$\begin{cases} -\mathbf{div}(\mathbb{C}\nabla_S(\mathbf{z}_i^\perp)) \overset{(42)}{=} -\mathbf{r}_{p,i}^\perp & \text{in } K \\ \mathbb{C}\nabla_S(\mathbf{z}_i^\perp)\mathbf{n} \overset{(42)}{=} \mathbf{0} & \text{on } \partial K, \end{cases} \tag{45}$$

elasticity problems. The rigid body motion components of the solutions to problems (44) and (45) are fixed, e.g., by the conditions

$$\int_{\partial K} \mathbf{z}_i \cdot \mathbf{r} = \int_{\partial K} \mathbf{u} \cdot \mathbf{r} \qquad \forall \mathbf{r} \in \mathbf{RM}(K),$$

where $\mathbf{u}$ can be chosen arbitrarily. In the following tests, we pick $\mathbf{u}$ as an element in $\mathbf{P}_p(K)$ such that its moments with respect to the elements of the basis of scaled monomials with maximum order p are equal to 1.

Step 3. We approximate the displacements, and thence the matrix $\mathbf{B}$, using a virtual element discretization as in [9] on the element K.

5.2 Stability constants on sequences of badly-shaped elements

We assess numerically the behaviour of the minimum (nonzero) and maximum eigenvalues for the generalized eigenvalue problem (40) for a fixed degree of accuracy on sequences of elements with increasing aspect ratio in two and three dimensions.

We consider both a compressible ($\lambda = \mu = 1$) and an incompressible materials ($\lambda = 10^5$, $\mu = 1$). For the computation of the matrix $\mathbf{B}$ in (43) we employ the VE scheme in [9]; as for the latter case, we further adopt a sub-integration of the divergence term, which leads to a locking free scheme.

First test case. We consider a sequence of elements as in Figure 1. The initial element is a nonconvex hexagon with hourglass shape; the distance between the two re-entrant vertices is 0.5, while that of the other couples of vertices is 1. The other elements are constructed by halving the distance between the two re-entrant corners at each step. We consider compressible materials.

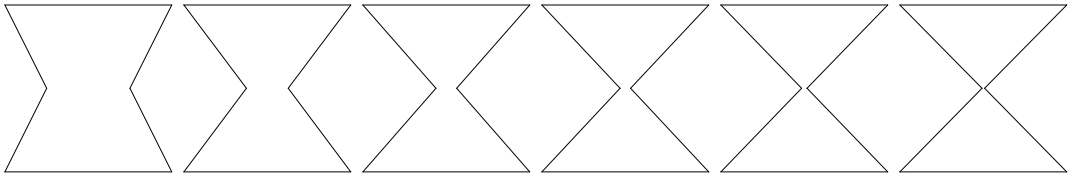

Figure 1: A sequence of 2D hourglass shaped elements for a compressible material.

Second test case. We consider a sequence of elements as in Figure 2. The initial element is a nonconvex decahedron with hourglass shape; the area of the upper and lower facets is 1, while that of the minimal square section is 1/4. The other elements are constructed by halving the size of the edges of the minimal square section. We consider compressible materials.

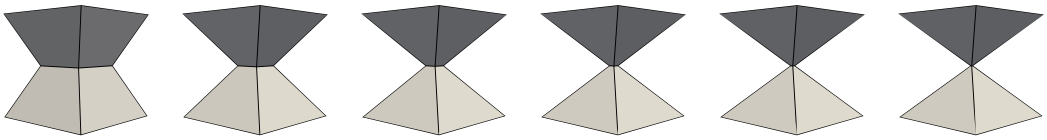

Figure 2: A sequence of 3D hourglass shaped elements for a compressible material.

Third test case. We consider a sequence of elements as in Figure 3. The initial element is an isosceles trapezoid, where the length of the top edge is 1/2 and that of the bottom edge is 1. The other elements are obtained by halving the distance between the bottom and top edges. We consider incompressible materials.

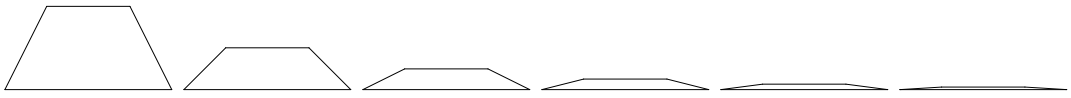

Figure 3: A sequence of 2D trapezoidal elements for an incompressible material.

Numerical results: minimum and maximum generalized eigenvalues. In Table 1, we display the minimum (nonzero) and maximum generalized eigenvalues of (40). For the 2D and 3D sequences of hourglass shaped elements in Figures 1and 2, we consider degree of accuracy $p = 1$; for the 2D sequences of trapezoidal elements in Figure 3, we set $p = 2$. We provide results for the projection-based (22) and the dofi-dofi (25) stabilizations $S^K(\cdot,\cdot)$ and $\widetilde{S}^K(\cdot,\cdot)$; in what follows, for the latter stabilization, we denote the matrix $\mathbf{A}$ by $\widetilde{\mathbf{A}}$.

From the results in Table 1, for the case of sequences of elements as in Figure 1, we observe that the minimum eigenvalues decrease moderately, while the maximum eigenvalues essentially do

Table 1 Minimum and maximum eigenvalues of (40) on sequences of badly-shaped elements.

	$S^K(\cdot,\cdot)$		$\widetilde{S}^K(\cdot,\cdot)$	
$p=1$	$\lrcorner_{min}$	$\lrcorner_{max}$	$\lrcorner_{min}$	$\lrcorner_{max}$
Fig. 1	1.0000e+00	2.7301e+02	3.4204e-01	2.7849e+02
	1.0000e+00	2.3326e+02	2.2719e-01	2.3492e+02
	6.4300e-01	2.0826e+02	1.7951e-01	2.0788e+02
	2.0247e-01	1.9905e+02	1.4982e-01	1.9722e+02
	7.8824e-02	1.9528e+02	6.7338e-02	1.9277e+02
	2.7496e-02	1.9338e+02	2.3740e-02	1.9065e+02
$p=1$	$\lrcorner_{min}$	$\lrcorner_{max}$	$\lrcorner_{min}$	$\lrcorner_{max}$
Fig. 2	1.2260e-01	7.5879e+04	1.2497e-01	5.6961e+04
	1.3380e-02	8.8178e+04	1.3875e-02	8.4101e+04
	1.9540e-03	9.6572e+04	2.0313e-03	9.9241e+04
	3.6127e-04	1.0486e+05	3.7564e-04	1.1105e+05
	8.1663e-05	1.1083e+05	8.4897e-05	1.1890e+05
	1.5835e-05	1.1373e+05	1.6496e-05	1.2314e+05
$p=2$	$\lrcorner_{min}$	$\lrcorner_{max}$	$\lrcorner_{min}$	$\lrcorner_{max}$
Fig. 3	1.9996e-05	6.5936e+02	1.9996e-05	6.7161e+02
	1.9980e-05	1.0625e+03	1.9980e-05	1.0757e+03
	1.9758e-05	1.4710e+03	1.9758e-05	1.4801e+03
	1.1262e-05	3.1641e+03	1.1262e-05	3.1704e+03
	2.0184e-10	2.3531e+03	2.0229e-10	2.3541e+03
	1.5359e-10	2.7322e+03	1.4313e-10	2.7215e+03

not increase; for the case of sequences of elements as in Figure 2, a less moderate growth of the maximum eigenvalues is displayed, while the minimum eigenvalues lose one order of magnitude at each halving step; for the case of sequences of elements as in Figure 3, the maximum eigenvalues grow slowly and the minimum eigenvalues are essentially constant, with the exception of the last two elements of the sequence; we shall motivate this behaviour in the next paragraph.

Numerical results: condition numbers. Under the same choices as in the previous paragraph, in Table 2, we assess the behaviour of the condition numbers of the matrices $\mathbf{A}$, $\widetilde{\mathbf{A}}$, and $\mathbf{B}$ in problem (40); we recall that the matrices $\mathbf{A}$ and $\widetilde{\mathbf{A}}$ are computed based on the projection-based (22) and dofi-dofi (25) stabilizations.

Table 2 Condition numbers of $\mathbf{A}$, $\widetilde{\mathbf{A}}$, and $\mathbf{B}$ in (40) on sequences of badly-shaped elements.

Fig. 1	$\mathbf{B}$	5.8348e+03	2.2734e+04	7.7885e+04	2.4295e+05	6.2642e+05	1.7875e+06
	$\mathbf{A}$	4.3858e+03	8.7185e+03	1.1033e+04	1.2342e+04	1.3042e+04	1.3395e+04
	$\widetilde{\mathbf{A}}$	3.4318e+03	6.3807e+03	7.4790e+03	7.9627e+03	8.1894e+03	8.2922e+03
Fig. 2	$\mathbf{B}$	3.4677e+04	9.3584e+04	2.0927e+05	5.4514e+05	2.3226e+06	2.5258e+07
	$\mathbf{A}$	9.9945e+03	1.8980e+04	2.6203e+04	3.0440e+04	3.2767e+04	3.3994e+04
	$\widetilde{\mathbf{A}}$	6.7282e+03	1.4792e+04	2.1655e+04	2.5956e+04	2.8424e+04	2.9758e+04
Fig. 3	$\mathbf{B}$	2.2076e+05	2.1286e+06	3.5757e+07	1.1220e+09	4.4996e+09	2.3369e+10
	$\mathbf{A}$	2.4149e+10	1.1371e+11	1.2118e+12	2.2248e+13	5.6501e+14	1.6530e+16
	$\widetilde{\mathbf{A}}$	1.3668e+10	6.9767e+10	9.0468e+11	1.9766e+13	5.4511e+14	1.6521e+16

From the results in Table 2, we deduce some facts: the condition numbers of $\mathbf{A}$ and $\widetilde{\mathbf{A}}$ are essentially the same, the latter being always slightly smaller than the former; there is no clear indication on whether the condition numbers of $\mathbf{B}$ are larger or smaller than those of $\mathbf{A}$ and $\widetilde{\mathbf{A}}$; the condition numbers for the last two trapezoidal elements are rather high, which suggests a reason why the corresponding minimum eigenvalues from the previous paragraph looked unreliable.

Table 3 Minimum and maximum eigenvalues of (40) for variable degrees of accuracy.

	$S^K(\cdot,\cdot)$		$\widetilde{S}^K(\cdot,\cdot)$	
p	$\lrcorner_{min}$	$\lrcorner_{max}$	$\lrcorner_{min}$	$\lrcorner_{max}$
1	1.0000e+00	1.7600e+02	2.6323e-01	1.7398e+02
2	9.9802e-01	5.9800e+02	4.3155e-01	5.7797e+02
3	9.9640e-01	1.2708e+03	9.3328e-01	1.2491e+03
4	9.9057e-01	2.3578e+03	9.9057e-01	2.3313e+03
5	9.6450e-01	4.1013e+03	9.6377e-01	4.0739e+03
6	9.3644e-01	6.8462e+03	9.3645e-01	6.8147e+03

5.3 Stability constants increasing the degree of accuracy

We assess numerically the behaviour of the minimum (nonzero) and maximum eigenvalues for the generalized eigenvalue problem (40) for increasing degree of accuracy on a fixed triangular element of vertices $(0,0)$, $(1,0)$, and $(0,1)$ in a compressible material; see Table 3. We provide results for the projection-based (22) and the dofi-dofi (25) stabilizations $S^K(\cdot,\cdot)$ and $\widetilde{S}^K(\cdot,\cdot)$.

From the results in Table 3, it appears that the minimum and maximum eigenvalues behave rather robustly with respect to the degree of accuracy.

6 Conclusions

For shape-regular sequences of polytopic meshes, we derived rigorously interpolation and stability estimates for HR-type virtual elements with fixed degree of accuracy in three dimensions (the two dimensional case is a low hanging fruit of the analysis given in this work). Essential tools in the analysis are integrations by parts, polynomial inverse estimates over suitable sub-tessellations of the polytopic elements, direct estimates, polynomial approximation results, and the proof of the well-posedness (with a priori estimates on the data involving constants that are explicit with respect to the shape of the domain) of mixed formulations of linear elasticity problems. Besides, we investigated on the numerical level the behaviour of the stabilization on sequences of badly-shaped elements and increasing degree of accuracy employing two different stabilizations: standard assumptions on the geometry are not enough to guarantee the robustness of the method. Future investigation will cope with the construction of ad-hoc stabilizations leading to stable bilinear forms on degenerating geometries and increasing degree of accuracy.

Acknowledgments. MB and LM have been partially funded by the European Union (ERC, NEMESIS, project number 101115663); views and opinions expressed are however those of the authors only and do not necessarily reflect those of the EU or the ERC Executive Agency. MB and MV have been partially funded by INdAM-GNCS project CUP_E53C23001670001. LM has been partially funded by MUR (PRIN2022 research grant n. 202292JW3F). GV and MV have been partially funded by MUR (PRIN2022 research grant n. 2022MBY5JM). GV has been partially funded by the Italian Ministry of Universities and Research (MUR) and the European Union through Next Generation EU, M4.C2.1.1, through the grant PRIN2022PNRR n. P2022M7JZW "SAFER MESH - Sustainable mAnagement oF watEr Resources ModEls and numerical MetHods" research grant, CUP H53D23008930001. All the authors are also members of the Gruppo Nazionale Calcolo Scientifico-Istituto Nazionale di Alta Matematica (GNCS-INdAM).

References

[1] S. Adams and B. Cockburn. A mixed finite element method for elasticity in three dimensions. *J. Sci. Comput.*, 25(3):515–521, 2005.

[2] D. N. Arnold and G. Awanou. Rectangular mixed finite elements for elasticity. *Math. Models Methods Appl. Sci.*, 15(09):1417–1429, 2005.

[3] D. N. Arnold, G. Awanou, and R. Winther. Finite elements for symmetric tensors in three dimensions. *Math. Comp.*, 77(263):1229–1251, 2008.

[4] D. N. Arnold and R. Winther. Mixed finite elements for elasticity. *Numer. Math.*, 92:401–419, 2002.

[5] E. Artioli, S. De Miranda, C. Lovadina, and L. Patruno. A stress/displacement virtual element method for plane elasticity problems. *Comput. Methods Appl. Mech. Engrg.*, 325:155–174, 2017.

[6] E. Artioli, S. De Miranda, C. Lovadina, and L. Patruno. A family of virtual element methods for plane elasticity problems based on the Hellinger–Reissner principle. *Comput. Methods Appl. Mech. Engrg.*, 340:978–999, 2018.

[7] A. K. Aziz, editor. *The mathematical foundations of the finite element method with applications to partial differential equations*. Academic Press, New York-London, 1972.

[8] L. Beirão da Veiga, F. Brezzi, A. Cangiani, G. Manzini, L.D. Marini, and A. Russo. Basic principles of virtual element methods. *Math. Models Methods Appl. Sci.*, 23(01):199–214, 2013.

[9] L. Beirão da Veiga, F. Brezzi, and L. D. Marini. Virtual elements for linear elasticity problems. *SIAM J. Numer. Anal.*, 51(2):794–812, 2013.

[10] D. Boffi, F. Brezzi, and M. Fortin. *Mixed finite element methods and applications*, volume 44. Springer, 2013.

[11] M. Botti and L. Mascotto. A Nečas-Lions inequality with symmetric gradients on star-shaped domains based on a first order Babuška-Aziz inequality. *J. Math. Anal. Appl.*, 545(2), 2025.

[12] L. Chen and J. Huang. Some error analysis on virtual element methods. *Calcolo*, 55(1):Paper No. 5, 23, 2018.

[13] L. Chen and X. Huang. A finite element elasticity complex in three dimensions. *Math. Comp.*, 91(337):2095–2127, 2022.

[14] S.-C. Chen and Y.-N. Wang. Conforming rectangular mixed finite elements for elasticity. *J. Sci. Comput.*, 47:93–108, 2011.

[15] S. H. Christiansen, J. Gopalakrishnan, J. Guzmán, and K. Hu. A discrete elasticity complex on three-dimensional Alfeld splits. *Numer. Math.*, 156(1):159–204, 2024.

[16] F. Dassi. Vem++, a c++ library to handle and play with the Virtual Element Method. `https://arxiv.org/abs/2310.05748`, 2023.

[17] F. Dassi, C. Lovadina, and M. Visinoni. A three-dimensional Hellinger-Reissner virtual element method for linear elasticity problems. *Comput. Methods Appl. Mech. Engrg.*, 364:112910, 17, 2020.

[18] D. A. Di Pietro and A. Ern. *Mathematical aspects of discontinuous Galerkin methods*, volume 69. Springer Science & Business Media, 2011.

[19] R. G. Durán. An elementary proof of the continuity from $L^2_0(\Omega)$ to $H^1_0(\Omega)^n$ of Bogovskii's right inverse of the divergence. *Rev. Un. Mat. Argentina*, 53(2):59–78, 2012.

[20] A. Ern and J.-L. Guermond. *Finite elements I: Approximation and interpolation*, volume 72. Springer Nature, 2021.

[21] S. Gong, J. Gopalakrishnan, J. Guzmán, and M. Neilan. Discrete elasticity exact sequences on Worsey–Farin splits. *ESAIM Math. Model. Numer. Anal.*, 57(6):3373–3402, 2023.

[22] J. Gopalakrishnan, J. Guzmán, and J. J. Lee. The Johnson-Mercier elasticity element in any dimensions. `https://arxiv.org/abs/2403.13189`, 2024.

[23] J. Guzmán and A. J. Salgado. Estimation of the continuity constants for Bogovskii and regularized Poincaré integral operators. *J. Math. Anal. Appl.*, 502(1):Paper No. 125246, 36, 2021.

[24] I. Hlaváček. Convergence of an equilibrium finite element model for plane elastostatics. *Aplikace Matematiky*, 24(6):427–457, 1979.

[25] J. Hu and S. Zhang. A family of symmetric mixed finite elements for linear elasticity on tetrahedral grids. *Sci. China Math.*, 58:297–307, 2015.

[26] C. Johnson and B. Mercier. Some equilibrium finite element methods for two-dimensional elasticity problems. *Numer. Math.*, 30:103–116, 1978.

[27] M. Křížek. An equilibrium finite element method in three-dimensional elasticity. *Aplikace Matematiky*, 27(1):46–75, 1982.

[28] L. Mascotto. The role of stabilization in the virtual element method: a survey. *Comput. Math. Appl.*, 151:244–251, 2023.

[29] W. C. H. McLean. *Strongly elliptic systems and boundary integral equations*. Cambridge university press, 2000.

[30] R. Verfürth. *A Posteriori Error Estimation Techniques for Finite Element Methods*. Numerical Mathematics and Scientific Computation. Oxford University Press, Oxford, 2013.

[31] M. Visinoni. A family of three-dimensional virtual elements for Hellinger-Reissner elasticity problems. *Comp. Math. Appl.*, 155:97–109, 2024.

[32] V. B. Watwood Jr. and B. J. Hartz. An equilibrium stress field model for finite element solutions of two-dimensional elastostatic problems. *Int. J. Solids Struct.*, 4(9):857–873, 1968.

A Well-posedness of the linear elasticity problem in mixed formulation with essential boundary conditions

We show a stability estimate for the Hellinger–Reissner formulation of linear elasticity problems with essential boundary conditions. We shall be able to prove a priori estimates that are explicit in terms of the ratio between the diameter and the radius of the largest ball with respect to which the domain is star-shaped. The main result of the appendix is Theorem A.7 below.

Strong formulation. Let Ω be a bounded, polyhedral, Lipschitz domain in $\mathbb{R}^3$, with boundary $\partial\Omega$ and outward unit normal vector $\mathbf{n}$. Given a volumetric force $\mathbf{f}$ in $\mathbf{L}^2(\Omega)$ and $\boldsymbol{\sigma}_N$ in $\mathbf{H}^{-\frac{1}{2}}(\partial\Omega)$, the linear elasticity problem in mixed formulation with an inhomogeneous, essential boundary condition reads as follows: Find a symmetric stress tensor $\underline{\boldsymbol{\sigma}}$ and a displacement field $\mathbf{u}$ such that

$$\begin{cases} -\mathbf{div}\ \underline{\boldsymbol{\sigma}} = \mathbf{f} & \text{in } \Omega \\ \underline{\boldsymbol{\sigma}} = \mathbb{C}\nabla_S \mathbf{u} & \text{in } \Omega \\ \underline{\boldsymbol{\sigma}}\mathbf{n} = \boldsymbol{\sigma}_N & \text{on } \partial\Omega. \end{cases} \tag{46}$$

On occasion, we shall be demanding extra regularity on the boundary condition, namely

$$\boldsymbol{\sigma}_N \in \mathbf{L}^2(\partial\Omega). \tag{47}$$

This is needed to derive explicit a priori estimates on the solution to (46). In what follows,

$$\begin{aligned} &h_\Omega \text{ denotes the diameter of } \Omega; \\ &\rho_\Omega \text{ denotes the radius of the largest ball with respect to which } \Omega \text{ is star-shaped.} \end{aligned} \tag{48}$$

A Stokes' lifting for the inhomogeneous essential condition. In order to write a weak formulation for (46), we construct a lifting of the essential condition $\boldsymbol{\sigma}_N$. To this aim, given the identity tensor $\mathbb{I}$, we consider the Stokes problem: Find a velocity field $\mathfrak{u}$ and a pressure $\mathfrak{p}$ such that

$$\begin{cases} -\mathbf{div}(\nabla_S \mathfrak{u} - \mathfrak{p}\ \mathbb{I}) = \mathbf{0} & \text{in } \Omega \\ \operatorname{div} \mathfrak{u} = 0 & \text{in } \Omega \\ (\nabla_S \mathfrak{u} - \mathfrak{p}\ \mathbb{I})\mathbf{n} = \boldsymbol{\sigma}_N & \text{on } \partial\Omega \\ \int_\Omega \mathfrak{u} = \mathbf{0}, \qquad \int_\Omega \nabla \times \mathfrak{u} = \mathbf{0}. \end{cases} \tag{49}$$

Introduce $\widetilde{\mathbf{H}}^1(\Omega)$ as the subspace of $\mathbf{H}^1(\Omega)$ consisting of fields $\mathfrak{v}$ satisfying the two conditions in the last line of (49).

A weak formulation of (49) reads

$$\begin{cases} \text{Find } (\mathfrak{u}, \mathfrak{p}) \in \mathfrak{V} \times \mathfrak{Q} := \widetilde{\mathbf{H}}^1(\Omega) \times L^2(\Omega) \text{ such that} & \\ (\nabla_S \mathfrak{u}, \nabla_S \mathfrak{v})_{0,\Omega} - (\operatorname{div} \mathfrak{v}, \mathfrak{p})_{0,\Omega} = \langle \boldsymbol{\sigma}_N, \mathfrak{v} \rangle & \forall \mathfrak{v} \in \mathfrak{V} \\ (\operatorname{div} \mathfrak{u}, \mathfrak{q})_{0,\Omega} = 0 & \forall \mathfrak{q} \in \mathfrak{Q}. \end{cases} \tag{50}$$

In order to prove the well-posedness of (50), we prove the two following technical results.

Lemma A.1 (Stokes' inf-sup condition)**.** *There exists a positive constant β_0, which only depends on the ratio between h_Ω and ρ_Ω in* (48) *such that*

$$\inf_{\mathfrak{q} \in \mathfrak{Q}} \sup_{\mathfrak{v} \in \mathfrak{V}} \frac{(\operatorname{div} \mathfrak{v}, \mathfrak{q})_{0,\Omega}}{|\mathfrak{v}|_{1,\Omega} \|\mathfrak{q}\|_{0,\Omega}} \geq \beta_0.$$

Proof. A lower bound for the constant β_0 is given, e.g., in [11, Proposition 1.1] in terms of the so-called Babuška-Aziz inequality [7]. In turns, an estimate for the constant appearing in that inequality (also known as the generalized Poincaré inequality), which is explicit in terms of the ratio between h_Ω and ρ_Ω in (48), is given in [23, Corollary 19, point 3]. □

Lemma A.2 (Korn's inequality)**.** *There exists a positive constant α_0, which only depends on the ratio between h_Ω and ρ_Ω in* (48)*, such that*

$$\alpha_0 \|\nabla \mathfrak{v}\|_{0,\Omega} \leq \|\nabla_S \mathfrak{v}\|_{0,\Omega} \qquad \forall \mathfrak{v} \in \mathfrak{V}. \tag{51}$$

Proof. We start by noting the splitting of the gradient into its symmetric (∇_S) and skew-symmetric (∇_{SS}) parts, and the identity

$$\|\nabla \mathfrak{v}\|_{0,\Omega}^2 = \|\nabla_S \mathfrak{v}\|_{0,\Omega}^2 + \|\nabla_{SS} \mathfrak{v}\|_{0,\Omega}^2.$$

It suffices to bound the second term on the right-hand side. Algebraic computations and the fact that $\mathfrak{v}$ belongs to $\widetilde{\mathbf{H}}^1(\Omega)$ (notably the fact that $\nabla \times \mathfrak{v}$ has zero average) imply that

$$\|\nabla_{SS} \mathfrak{v}\|_{0,\Omega} = \frac{1}{\sqrt{2}} \|\nabla \times \mathfrak{v}\|_{0,\Omega} = \frac{1}{\sqrt{2}} \inf_{\mathbf{c} \in \mathbb{R}^3} \|\nabla \times \mathfrak{v} - \mathbf{c}\|_{0,\Omega}.$$

A Nečas-Lions inequality holds true using, e.g., [19, Theorem 3.2], with a constant $C_{NL,0}$ only depending on the ratio between h_Ω and ρ_Ω in (48) such that

$$\inf_{\mathbf{c} \in \mathbb{R}^3} \|\nabla \times \mathfrak{v} - \mathbf{c}\|_{0,\Omega} \leq C_{NL,0} \|\nabla(\nabla \times \mathfrak{v})\|_{-1,\Omega}.$$

Algebraic computations as in [11, Lemma 3.1] and manipulations on negative Sobolev norms entail

$$\|\nabla(\nabla \times \mathfrak{v})\|_{-1,\Omega} \leq 2 \|\nabla \times (\nabla_S \mathfrak{v})\|_{-1,\Omega} \leq 2 \|\nabla_S \mathfrak{v}\|_{0,\Omega}.$$

Combining the above displays yields the assertion. □

We deduce the well-posedness of problem (50).

Proposition A.3. *Problem* (50) *is well-posed. Given* $(\mathfrak{u}, \mathfrak{p})$ *the solutions to* (50)*, there exists a positive constant c_L such that*

$$|\mathfrak{u}|_{1,\Omega} + \|\mathfrak{p}\|_{0,\Omega} \leq c_L \|\boldsymbol{\sigma}_N\|_{-\frac{1}{2},\partial\Omega}. \tag{52}$$

If assumption (47) *holds true, then there exists a positive constant $\widetilde{c}_L$ only depending on the ratio between h_Ω and ρ_Ω in* (48) *such that*

$$|\mathfrak{u}|_{1,\Omega} + \|\mathfrak{p}\|_{0,\Omega} \leq \widetilde{c}_L \|\boldsymbol{\sigma}_N\|_{0,\partial\Omega}. \tag{53}$$

Proof. Existence and uniqueness of a solution to (50) are a consequence of the standard inf-sup theory, and Lemmas A.1 and A.2.

As for the stability estimates, we focus first on the case $\boldsymbol{\sigma}_N$ only belongs to $\mathbf{H}^{-\frac{1}{2}}(\partial D)$. We take $\mathfrak{v} = \mathfrak{u}$ and $\mathfrak{q} = \mathfrak{p}$ in (50) and deduce

$$\|\nabla_S \mathfrak{u}\|_{0,\Omega}^2 = \langle \boldsymbol{\sigma}_N, \mathfrak{u} \rangle \leq \|\boldsymbol{\sigma}_N\|_{-\frac{1}{2},\partial\Omega} \|\mathfrak{u}\|_{\frac{1}{2},\partial\Omega}.$$

The standard trace inequality [20, Theorem 3.10, point (iii)], the Poincaré inequality [20, Lemma 3.24], and Korn's inequality (51) entail the existence of a positive C such that

$$\|\nabla_S \mathfrak{u}\|_{0,\Omega} \leq C \|\boldsymbol{\sigma}_N\|_{-\frac{1}{2},\partial\Omega}.$$

We are not able to detect an explicit dependence of C on the ratio between h_Ω and ρ_Ω in (48), due to the use of the standard trace inequality. Combining the above bounds yields the bound on $|\mathfrak{u}|_{1,\Omega}$ in (52). The bound on $\|\mathfrak{p}\|_{0,\Omega}$ follows from the standard inf-sup theory.

We now prove (53) under assumption (47). We take $\mathfrak{v} = \mathfrak{u}$ and $\mathfrak{q} = \mathfrak{p}$ in (50), and deduce

$$\|\nabla_S \mathfrak{u}\|_{0,\Omega}^2 = \langle \boldsymbol{\sigma}_N, \mathfrak{u} \rangle \leq \|\boldsymbol{\sigma}_N\|_{0,\partial\Omega} \|\mathfrak{u}\|_{0,\partial\Omega}.$$

The continuous trace inequality [18, Lemma 1.49] (constant c_{cti}), the Poincaré inequality [20, Lemma 3.24] (constant c_P), and Korn's inequality (51) (constant α_0) give

$$\|\nabla_S \mathfrak{u}\|_{0,\Omega} \leq c_{cti}\ c_P\ \alpha_0 \|\boldsymbol{\sigma}_N\|_{0,\partial\Omega}.$$

The three constants in the display above are explicit with respect to the ratio between h_Ω and ρ_Ω in (48). The bound on $|\mathfrak{u}|_{1,\Omega}$ in (52) is proven. We are left with the bound on $\|\mathfrak{p}\|_{0,\Omega}$, which indeed follows from [10, Theorem 4.2.3], and the fact that α_0, $C_{\mathfrak{a}}$, and β_0 are explicit with respect to the ratio between h_Ω and ρ_Ω in (48). □

We are now in a position to define a stable lifting $\widehat{\underline{\boldsymbol{\sigma}}}$ of $\boldsymbol{\sigma}_N$. Given $(\mathfrak{u}, \mathfrak{p})$ the solution to (50), we introduce the symmetric tensor

$$\widehat{\underline{\boldsymbol{\sigma}}} := \nabla_S \mathfrak{u} - \mathfrak{p}\, \mathbb{I}. \tag{54}$$

The triangle inequality and Proposition A.3 yield

$$\|\widehat{\underline{\boldsymbol{\sigma}}}\|_{0,\Omega} \leq \widetilde{c}_L \|\boldsymbol{\sigma}_N\|_{0,\partial\Omega}, \tag{55}$$

where $\widetilde{c}_L$ is the constant in (53). Moreover, problem (49) implies that $\widehat{\underline{\boldsymbol{\sigma}}}$ is divergence free.

A weak formulation of (46). Let $\underline{\boldsymbol{\Sigma}}$, $\mathbf{V}$, and $a(\cdot,\cdot)$ be as in (5). Given $\widehat{\underline{\boldsymbol{\sigma}}}$ as in (54), an equivalent weak formulation of (46) reads as follows:

$$\begin{cases} \text{Find } \underline{\boldsymbol{\sigma}}_0 \in \underline{\boldsymbol{\Sigma}} \text{ and } \mathbf{u} \in \mathbf{V} \text{ such that} & \\ a(\underline{\boldsymbol{\sigma}}_0, \underline{\boldsymbol{\tau}}) + (\mathbf{div}\, \underline{\boldsymbol{\tau}}, \mathbf{u})_{0,\Omega} = -a(\widehat{\underline{\boldsymbol{\sigma}}}, \underline{\boldsymbol{\tau}}) & \forall \underline{\boldsymbol{\tau}} \in \underline{\boldsymbol{\Sigma}} \\ (\mathbf{div}\, \underline{\boldsymbol{\sigma}}_0, \mathbf{v})_{0,\Omega} = -(\mathbf{f}, \mathbf{v})_{0,\Omega} & \forall \mathbf{v} \in \mathbf{V}. \end{cases} \tag{56}$$

The solution $\underline{\boldsymbol{\sigma}}$ to (46) is given by the sum of $\underline{\boldsymbol{\sigma}}_0$ and $\widehat{\underline{\boldsymbol{\sigma}}}$. Below, under assumption (47), we shall discuss the well-posedness of (56), and derive a priori estimates for $\underline{\boldsymbol{\sigma}}$, which are explicit with respect to the ratio between h_Ω and ρ_Ω in (48).

The well-posedness for the case of natural and mixed natural-essential boundary conditions is discussed in [10, Chapter 8], yet without an explicit knowledge of the constants in the a priori estimates.

A technical result. We prove a result, which is instrumental to infer the coercivity on the kernel of the bilinear form $a(\cdot,\cdot)$ employed in (56).

Lemma A.4. *There exists a positive constant C_d only depending on the ratio between h_Ω and ρ_Ω in* (48) *such that*

$$\|\underline{\boldsymbol{\tau}}\|_{0,\Omega} \leq C_d \left(\|\mathbf{dev}\, \underline{\boldsymbol{\tau}}\|_{0,\Omega} + h_\Omega \|\mathbf{div}\, \underline{\boldsymbol{\tau}}\|_{0,\Omega} \right) \qquad \forall \underline{\boldsymbol{\tau}} \in \underline{\boldsymbol{\Sigma}}. \tag{57}$$

Proof. Using [23, Corollary 19, point 3], there exists a positive constant c_{GS} only depending on h_Ω and ρ_Ω such that for any $\underline{\boldsymbol{\tau}}$ in $\underline{\boldsymbol{\Sigma}}$, there exists $\mathbf{v}$ in $\mathbf{H}^1(\Omega) \cap \mathbf{L}^2_0(\Omega)$ satisfying

$$\operatorname{div} \mathbf{v} = \operatorname{tr}(\underline{\boldsymbol{\tau}}) \quad \text{and} \quad |\mathbf{v}|_{1,\Omega} \leq c_{GS} \|\operatorname{tr}(\underline{\boldsymbol{\tau}})\|_{0,\Omega}. \tag{58}$$

The definition of the **dev** operator allows us to write

$$\int_\Omega \operatorname{tr}(\underline{\boldsymbol{\tau}})^2 = \int_\Omega \operatorname{tr}(\underline{\boldsymbol{\tau}}) \operatorname{div} \mathbf{v} = \int_\Omega \underline{\boldsymbol{\tau}} : \operatorname{tr}(\nabla \mathbf{v}) \mathbb{I} = 3 \int_\Omega \underline{\boldsymbol{\tau}} : (\nabla \mathbf{v} - \mathbf{dev}(\nabla \mathbf{v})).$$

Using the symmetry of $\underline{\boldsymbol{\tau}}$, an integration by parts, the above identity, the definition of $\underline{\boldsymbol{\Sigma}}$ in (5), the Cauchy–Schwarz inequality, the Poincaré inequality [20, Section 3.3] (constant c_P independent of the ratio between h_Ω and ρ_Ω in (48)), and (58) (constant c_{GS}), we get

$$\begin{aligned} \|\operatorname{tr}(\underline{\boldsymbol{\tau}})\|^2_{0,\Omega} &= -3 \int_\Omega \mathbf{dev}\, \underline{\boldsymbol{\tau}} : \nabla_S \mathbf{v} - 3 \int_\Omega (\mathbf{div}\, \underline{\boldsymbol{\tau}}) \cdot \mathbf{v} \\ &\leq 3 \left(\|\mathbf{dev}\, \underline{\boldsymbol{\tau}}\|_{0,\Omega} \|\nabla_S \mathbf{v}\|_{0,\Omega} + \|\mathbf{div}\, \underline{\boldsymbol{\tau}}\|_{0,\Omega} \|\mathbf{v}\|_{0,\Omega} \right) \\ &\leq (1 + c_P) \left(\|\mathbf{dev}\, \underline{\boldsymbol{\tau}}\|_{0,\Omega} + h_\Omega \|\mathbf{div}\, \underline{\boldsymbol{\tau}}\|_{0,\Omega} \right) |\mathbf{v}|_{1,\Omega} \\ &\leq (1 + c_P) c_{GS} \left(\|\mathbf{dev}\, \underline{\boldsymbol{\tau}}\|_{0,\Omega} + h_\Omega \|\mathbf{div}\, \underline{\boldsymbol{\tau}}\|_{0,\Omega} \right) \|\operatorname{tr}(\underline{\boldsymbol{\tau}})\|_{0,\Omega}. \end{aligned}$$

We deduce

$$\|\operatorname{tr}(\underline{\boldsymbol{\tau}})\|_{0,\Omega} \leq (1 + c_P) c_{GS} \left(\|\mathbf{dev}\, \underline{\boldsymbol{\tau}}\|_{0,\Omega} + h_\Omega \|\mathbf{div}\, \underline{\boldsymbol{\tau}}\|_{0,\Omega} \right).$$

The assertion follows using again the definition of the **dev** operator:

$$\|\underline{\boldsymbol{\tau}}\|_{0,\Omega} \leq \|\mathbf{dev}\, \underline{\boldsymbol{\tau}}\|_{0,\Omega} + \|\operatorname{tr}(\underline{\boldsymbol{\tau}})\|_{0,\Omega} \leq 2(1 + c_P) c_{GS} \left(\|\mathbf{dev}\, \underline{\boldsymbol{\tau}}\|_{0,\Omega} + h_\Omega \|\mathbf{div}\, \underline{\boldsymbol{\tau}}\|_{0,\Omega} \right).$$

□

An inf-sup condition and coercivity on the kernel for the Hellinger–Reissner principle. We recall an inf-sup condition for the Hellinger–Reissner principle, whose proof can be found in [11, Proposition 1.5].

Proposition A.5. *There exists a positive constant β_0^* only depending on the ratio of h_Ω and ρ_Ω such that*

$$\inf_{\mathbf{v}\in\mathbf{V}} \sup_{\underline{\boldsymbol{\tau}}\in\underline{\boldsymbol{\Sigma}}} \frac{(\mathbf{div}\,\underline{\boldsymbol{\tau}},\mathbf{v})_{0,\Omega}}{\|\underline{\boldsymbol{\tau}}\|_{\underline{\boldsymbol{\Sigma}}}\|\mathbf{v}\|_{\mathbf{V}}} \geq h_\Omega^{-1}\beta_0^*. \tag{59}$$

We define the Hellinger–Reissner kernel as

$$\mathbb{K} := \{\underline{\boldsymbol{\tau}} \in \underline{\boldsymbol{\Sigma}} \mid (\mathbf{div}\,\underline{\boldsymbol{\tau}},\mathbf{v})_{0,\Omega} = 0 \quad \forall \mathbf{v}\in\mathbf{V}\}. \tag{60}$$

Proposition A.6. *The coercivity of $a(\cdot,\cdot)$ on the kernel $\mathbb{K}$*

$$\alpha_0^*\|\underline{\boldsymbol{\tau}}\|_{\underline{\boldsymbol{\Sigma}}}^2 \leq a(\underline{\boldsymbol{\tau}},\underline{\boldsymbol{\tau}}) \qquad\qquad \forall \underline{\boldsymbol{\tau}}\in\mathbb{K} \tag{61}$$

holds true with coercivity constant a_0^* independent of the ratio between h_Ω and ρ_Ω in (48)*, and the Lamé parameter λ.*

Proof. We have

$$a(\underline{\boldsymbol{\tau}},\underline{\boldsymbol{\tau}}) \geq (2\mu)^{-1}\|\mathbf{dev}\,\underline{\boldsymbol{\tau}}\|_{0,\Omega}^2 \overset{(57),(60)}{\geq} (2\mu C_d)^{-1}\|\underline{\boldsymbol{\tau}}\|_{0,\Omega}^2 \overset{(60)}{=} (2\mu C_d)^{-1}\|\underline{\boldsymbol{\tau}}\|_{\underline{\boldsymbol{\Sigma}}}^2 \qquad \forall \underline{\boldsymbol{\tau}}\in\mathbb{K}. \tag{62}$$

□

Well posedness of (56)**.** We are in a position to prove the main result of the appendix.

Theorem A.7. *For every $\mathbf{f}$ in $\mathbf{L}^2(\Omega)$, $\boldsymbol{\sigma}_N$ in $\mathbf{L}^2(\partial\Omega)$, and $\widehat{\underline{\boldsymbol{\sigma}}}$ as in* (54)*, problem* (56) *admits a unique solution $(\underline{\boldsymbol{\sigma}},\mathbf{u})$ in $\underline{\boldsymbol{\Sigma}}\times\mathbf{V}$. Moreover, there exists a positive constant c_{HR} depending on the ratio between h_Ω and ρ_Ω in* (48)*, and μ, but independent of λ such that the solution to problem* (56) *satisfies the stability bound*

$$\|\underline{\boldsymbol{\sigma}}\|_{\underline{\boldsymbol{\Sigma}}} + \|\mathbf{u}\|_{\mathbf{V}} \leq c_{HR}(\|\mathbf{f}\|_{0,\Omega} + \|\boldsymbol{\sigma}_N\|_{0,\partial\Omega}).$$

If assumption (47) *is not valid, well-posedness can be still proved but without an explicit dependence of the stability constant in terms of the geometric properties of Ω.*

Proof. Since the right-hand sides in (56) define linear functionals on $\underline{\boldsymbol{\Sigma}}$ and $\mathbf{V}$, existence and uniqueness of the solution to (56) follow from the standard inf-sup theory, (59), and (62).

From [10, eqs. (4.2.36) and (4.2.37)], the constant in a priori estimates only depend on the continuity constants of the two bilinear forms and the right-hand side, the inf-sup constant β_0^* in (59), and the coercivity constant α_0^* in (61). All such constants are independent of h_Ω and ρ_Ω; see Propositions A.5 and A.6. On the other hand, the right-hand side involves the lifting $\widehat{\underline{\boldsymbol{\sigma}}}$ of the essential boundary condition $\boldsymbol{\sigma}_N$. Under assumption (47), we can further use (55) and deduce the assertion. □

MOX Technical Reports, last issues

Dipartimento di Matematica
Politecnico di Milano, Via Bonardi 9 - 20133 Milano (Italy)

09/2025 Quarteroni, A.; Gervasio, P.; Regazzoni, F.
Combining physics-based and data-driven models: advancing the frontiers of research with Scientific Machine Learning

08/2025 Botti, M.; Fumagalli, I.; Mazzieri, I.
Polytopal discontinuous Galerkin methods for low-frequency poroelasticity coupled to unsteady Stokes flow

07/2025 Patanè, G.; Nicolussi, F.; Krauth, A.; Gauglitz, G.; Colosimo, B. M.; Dede', L.; Menafoglio, A.
Functional-Ordinal Canonical Correlation Analysis With Application to Data from Optical Sensors

06/2025 Torzoni, M.; Manzoni, A.; Mariani, A.
Enhancing Bayesian model updating in structural health monitoring via learnable mappings

04/2025 Andrini, D.; Magri, M.; Ciarletta, P.
Nonlinear morphoelastic theory of biological shallow shells with initial stress

05/2025 Buchwald, S.; Ciaramella, G.; Verani, M.
Greedy reconstruction algorithms for function approximation

02/2025 Corda, A.; Pagani, S.; Vergara, C.
Influence of patient-specific acute myocardial ischemia maps on arrhythmogenesis: a computational study

01/2025 Dede', L.; Parolini, N.; Quarteroni, A.; Villani, G.; Ziarelli, G.
SEIHRDV: a multi-age multi-group epidemiological model and its validation on the COVID-19 epidemics in Italy

110/2024 Pederzoli, V.; Corti, M.; Riccobelli, D.; Antonietti, P.F.
A coupled mathematical and numerical model for protein spreading and tissue atrophy, applied to Alzheimer's disease

109/2024 Liverotti, L.; Ferro, N.; Matteucci, M.; Perotto, S.
A PCA and mesh adaptation-based format for high compression of Earth Observation optical data with applications in agriculture